

Design and Structure–Activity Relationship of a New Class of Potent VEGF Receptor Tyrosine Kinase Inhibitors

Laurent F. Hennequin,^{*,†} Andrew P. Thomas,[‡] Craig Johnstone,[‡] Elaine S. E. Stokes,[‡] Patrick A. Plé,[†] Jean-Jacques M. Lohmann,[†] Donald J. Ogilvie,[‡] Mike Dukes,[‡] Steve R. Wedge,[‡] Jon O. Curwen,[‡] Jane Kendrew,[‡] and Christine Lambert-van der Brempt[†]

AstraZeneca, Zeneca Pharma, Centre de Recherches, Z.I. La Pompelle, B.P. 1050, Chemin de Vrilly, 51689 Reims Cedex 2, France, and AstraZeneca Pharmaceuticals, Alderley Park, Macclesfield, Cheshire SK10 4TG, United Kingdom

Received July 6, 1999

A series of substituted 4-anilinoquinazolines and related compounds were synthesized as potential inhibitors of vascular endothelial growth factor (VEGF) receptor (Flt and KDR) tyrosine kinase activity. Enzyme screening indicated that a narrow structure–activity relationship (SAR) existed for the bicyclic ring system, with quinazolines, quinolines, and cinnolines having activity and with quinazolines and quinolines generally being preferred. Substitution of the aniline was investigated and clearly indicated that small lipophilic substituents such as halogens or methyl were preferred at the C-4' position. Small substituents such as hydrogen and fluorine are preferred at the C-2' position. Introduction of a hydroxyl group at the meta position of the aniline produced the most potent inhibitors of Flt and KDR tyrosine kinases activity with IC₅₀ values in the nanomolar range (e.g. **10**, **12**, **13**, **16**, and **18**). Investigation of the quinazoline C-6 and C-7 positions indicates that a large range of substituents are tolerated at C-7, whereas variation at the C-6 is more restricted. At C-7, neutral, basic, and heteroaromatic side chains led to very potent compounds, as illustrated by the methoxyethoxy derivative **13** (IC₅₀ < 2 nM). Our inhibitors proved to be very selective inhibitors of Flt and KDR tyrosine kinase activity when compared to that associated with the FGF receptor (50- to 3800-fold). Observed enzyme profiles translated well with respect to potency and selectivity for inhibition of growth factor stimulated proliferation of human umbilical vein endothelial cells (HUVECs). Oral administration of selected compounds to mice produced total plasma levels 6 h after dosing of between 3 and 49 μM. In vivo efficacy was demonstrated in a rat uterine oedema assay where significant activity was achieved at 60 mg/kg with the meta hydroxy anilinoquinazoline **10**. Inhibition of growth of human tumors in athymic mice has also been demonstrated: compound **34** inhibited the growth of established Calu-6 lung carcinoma xenograft by 75% (*P* < 0.001, one tailed t-test) following daily oral administration of 100 mg/kg for 21 days.

Introduction

Pathological angiogenesis has been associated with a variety of disease states including diabetic retinopathy, psoriasis, cancer, rheumatoid arthritis, atheroma, Kaposi's sarcoma, and haemangioma.^{1,2} Altered vascular permeability is also thought to play a role in such processes.^{3,4,5}

Several polypeptides with in vitro endothelial cell growth promoting activity have been identified, including acidic and basic fibroblast growth factors (aFGF bFGF) and vascular endothelial growth factor (VEGF). By virtue of the restricted expression of its receptors, the growth factor activity of VEGF, in contrast to that of the FGFs, is relatively specific toward endothelial cells. Recent evidence indicates that VEGF is an important stimulator of both normal and pathological angiogenesis.^{6–10} VEGF has been shown to be secreted by human tumor cell lines in culture (e.g. glioma¹¹ and melanoma¹²). Moreover VEGF protein as well as mRNA

for the VEGF receptors Flk-1/KDR have been identified in primary tumors of breast,^{13,14} colon,^{15,16} and renal origin.¹⁷

Receptor tyrosine kinases (RTKs) have been shown to be important mediators of signal transduction in cells.^{8,9,18–20} These transmembrane molecules characteristically consist of an extracellular ligand-binding domain connected through a segment in the plasma membrane to an intracellular tyrosine kinase domain. Binding of the ligand to the receptor results in receptor dimerization and stimulation of the receptor-associated tyrosine kinase activity, which leads to phosphorylation of tyrosine residues on both the receptor and other intracellular molecules. These changes in tyrosine phosphorylation initiate a signaling cascade leading to a variety of cellular responses. Two endothelium associated, high-affinity RTKs for VEGF have been identified, the fms-like tyrosine kinase receptor, Flt, and the kinase insert domain-containing receptor, KDR (also referred to as Flk-1 in mice).^{21,22}

Blockade of VEGF signal transduction by sequestration of VEGF with antibody has been shown to prevent tumor growth.²³ VEGF RTKs must, therefore, be viewed as attractive therapeutic targets for the development

* Corresponding author. Phone: 33-3-26-61-68-49. Fax: 33-3-26-61-68-42.

[†] AstraZeneca, Zeneca Pharma.

[‡] AstraZeneca Pharmaceuticals.

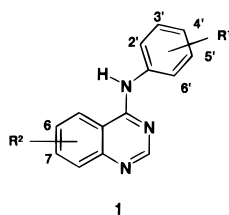


Figure 1.

of novel agents to treat angioproliferative diseases such as cancer.^{9,10}

Recently, a series of substituted indolin-2-ones that inhibits RTKs has been reported, some of which are micromolar inhibitors of Flk-1.²⁴

In this paper, we describe the synthesis and structure–activity relationships (SAR) for inhibition of tyrosine phosphorylation by anilinoquinazolines **1** (Figure 1), a novel series of extremely potent submicromolar inhibitors of VEGF receptor tyrosine kinases. Selected analogues were also evaluated *in vivo* in a rat uterine oedema model and for inhibition of growth of human lung carcinoma xenograft (Calu-6) in athymic mice. We also discuss a possible binding mode for these inhibitors in the catalytic domain of the VEGF RTK, based on the generated SAR and the published structural data on protein kinases.

Chemistry

The 6,7-dimethoxyanilinoquinazolines **2–10** (Table 1) have been prepared by multiparallel synthesis by refluxing the 4-chloroquinazoline **38**²⁵ with commercially available anilines in 2-propanol as described in Scheme 1.

Anilinoquinazolines possessing C-6 and C-7 substituents different from the methoxy group described in Tables 1–3 were prepared by two general strategies based on the same intermediate, namely the 7-benzyloxy-3,4-dihydroquinazolin-4-one **40**, obtained by refluxing the aminobenzamide derivative **39**²⁶ with Gold's reagent in dioxane (Scheme 2). In the first approach (Scheme 2, steps c–h), the anilines were coupled to the quinazolinone nucleus prior to the introduction of the C-7 side chains as follows: chlorination of **40** using thionyl chloride gave the 7-benzyloxy-4-chloroquinazolinone **41**. Nucleophilic displacement of the chlorine atom of **41** with anilines yielded the corresponding 7-benzyloxy-4-anilinoquinazolines **42–45**. Cleavage of the C-7 benzyl protecting group with either TFA or by hydrogenation using 10% Pd on charcoal led to the corresponding unprotected C-7 hydroxy-4-anilinoquinazolines **47–50**.

The C-7 side chains were then introduced (Scheme 2, steps g and h), either by direct alkylation of the phenol moiety with commercially available chloroalkyl or chloroaryl derivatives in DMF in the presence of potassium carbonate or by the Mitsunobu reaction using DEAD, triphenylphosphine (or *n*-butylphosphine/ADDP) in the presence of an alcohol derivative. In the case of the meta-hydroxy derivative **45**, the hydroxyl on the aniline was protected prior to the C-7 alkylation. The carbonate group was selected for this purpose due to its stability in the neutral conditions of the Mitsunobu reaction and lability under basic conditions, giving rise to **46**. After introduction of the C-7 substituent, the

meta-hydroxyl function was liberated using aqueous sodium hydroxide to give **13**.

The second approach involved the introduction of the C-7 chain prior to attachment of the aniline ring (Scheme 2, steps i–n). The quinazolinone **40** was protected on N-3 using a pivaloyloxymethyl (POM) group to give **51**. Cleavage of the C-7 benzyl group was achieved by hydrogenation to give the phenol **52**. Introduction of the C-7 side chains used similar conditions to those in the first approach to give the C-7-methoxyethoxy derivative **53** and C-7-ethoxytriazole derivative **54**. Cleavage of the POM protecting group under basic conditions led respectively to the free quinazolinones **55** and **57**. Subsequent chlorination with thionyl chloride gave the corresponding C-4 chloroquinazolines **56** and **58**. Displacement of the C-4 halogen atom of the hydrochloride salt of the chloroquinazolines with anilines in protic solvent (2-propanol) led to the expected anilinoquinazolines **12** and **36** (Scheme 2).

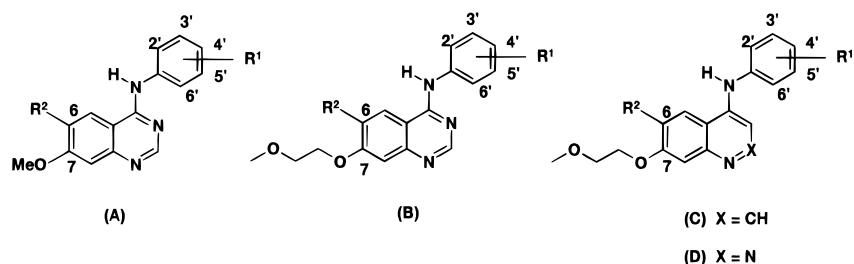
The disubstituted derivative **14** (Scheme 3) was prepared by reacting **47** with pyridine hydrochloride to release the free catechol **59** followed by the double alkylation of the resulting C-6 and C-7 free hydroxyl using commercially available bromoethyl methyl ether in the presence of potassium carbonate in DMF (Scheme 3).

The amides **31** and **33** were obtained as described in Scheme 4. The commercially available N-protected nitro-benzamide **60** was deacylated under acidic conditions to give the anthranilic acid **61**. Reaction of **61** with formamide led to the corresponding nitroquinazolinone **62**, which was then chlorinated (SOCl₂, DMF) to give **63**. This product was reacted with the 2-fluoro-4-chloro aniline or with the 2-fluoro-4-methyl-5-methoxy-carbo-nyloxy aniline to give respectively **64** and **65**. Reduction of the C-7 nitro moiety followed by acylation of the resulting amine with methoxyacetyl chloride in pyridine gave **31** and **68**. The meta-hydroxy compound **33** was obtained from **68**, after hydrolysis with aqueous sodium hydroxide.

The monosubstituted C-7-methoxyethoxy derivative **15** was obtained from the fluoroquinazolinone **69**²⁷ by displacement of the fluorine with 2-methoxyethoxide to give **70**, which was in turn chlorinated and further reacted with the 2-fluoro-4-chloro aniline (Scheme 5).

The morpholinobutoxy derivative **23** was obtained by coupling 1-bromo-4-chlorobutane with **47** to give **72** followed by the displacement of the chlorine atom of **72** with morpholine (Scheme 6).

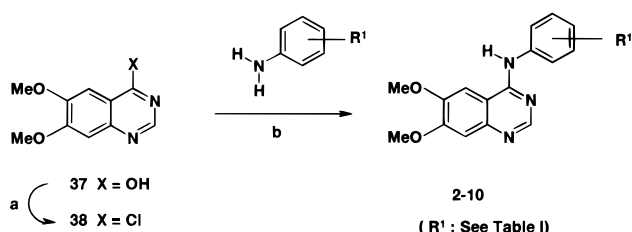
The 4-anilinoquinolines **16** and **17** and the 4-anilino-cinnolines **18** and **19** (Scheme 7) were prepared from **78** and **83**, following a strategy similar to the first procedure used in the anilinoquinazolinone series. The intermediate chloroquinoline **78** was obtained from 2-methoxy-4-nitrophenol **79** by successive alkylation with 1-bromo-2-methoxyethane followed by hydrogenation of the nitro function to give the aniline **81**. Reaction of **81** with diethylethoxymethylene malonate at 110 °C led to the intermediate aryl-enamines, which was in turn cyclized to the quinolinone **77** by a thermal decarboxylation/cyclization reaction in diphenyl ether. Finally, chlorination of **77** using standard conditions (thionyl chloride) gave the chloroquinoline **78**. A similar sequence was used to prepare the cinnolinone derivative

Table 1. Role of the Nucleus and Aniline Substitution on Enzyme Inhibition and Enzyme Selectivity

no.	series	R1				R2	procedure	formula ^a	enzyme inhibition @ 2 μM ATP concentration IC ₅₀ μM ^b			enzyme selectivity IC ₅₀ ratios	
		2'	3'	4'	5'				Flt	KDR	FTK	FTK/Flt	FTK/KDR
2	A	F	H	H	H	MeO	A	C ₁₆ H ₁₄ O ₂ N ₃ F·1.1 HCl, 0.1 H ₂ O	26	2.7	>100	>4	>35
3	A	H	H	Cl	H	MeO	A	C ₁₆ H ₁₄ O ₂ N ₃ Cl·1.1 HCl	11	0.8	>100	>9	>120
4	A	F	H	Cl	H	MeO	A	C ₁₆ H ₁₃ O ₂ N ₃ FCI·1.23 HCl	2.0	0.1	7	~4	70
5	A	H	OH	H	H	MeO	A	C ₁₆ H ₁₅ O ₃ N ₃ ·1.0 HCl, 0.5 H ₂ O	0.2	0.05	11	>50	>200
6	A	F	H	I	H	MeO	A	C ₁₆ H ₁₃ O ₂ N ₃ FI·0.88 HCl, 0.7 H ₂ O	0.8				
7	A	Cl	H	I	H	MeO	A	C ₁₆ H ₁₃ O ₂ N ₃ CI·1.1 HCl	>33				
8	A	F	H	F	H	MeO	A	C ₁₆ H ₁₃ O ₂ N ₃ F ₂ ·1.2 HCl, 0.2 H ₂ O	22	2.9	58	~3	~20
9	A	H	Cl	F	H	MeO	A	C ₁₆ H ₁₃ O ₂ N ₃ FCI·1.2 HCl, 0.26 H ₂ O	>100	0.8	>100		>120
10	A	F	H	Me	OH	MeO	A	C ₁₇ H ₁₆ N ₃ FO ₃ ·1 HCl, 0.65 iPrOH	0.03	0.003	2.5	~80	>800
11	B	F	H	Cl	H	MeO	B	C ₁₈ H ₁₇ N ₃ O ₃ ClF·1.0 HCl	0.4	0.007	27	>65	>3800
12	B	H	OH	H	H	MeO	A	C ₁₈ H ₁₉ O ₄ N ₃ ·1.1 HCl, 0.23 H ₂ O	0.03	<0.005	7	>200	>1400
13	B	F	H	Cl	OH	MeO		C ₁₈ H ₁₇ N ₃ ClFO ₄ ·1.6 H ₂ O	<0.002	<0.002	7.4	>3600	>3600
14	B	F	H	Cl	H	MeO(CH ₂) ₂ O	B	C ₂₀ H ₂₁ ClFN ₃ O ₄ ·1 HCl	0.9	0.06	>100	>100	>1600
15	B	F	H	Cl	H	H	C	C ₁₇ H ₁₅ N ₃ O ₂ FCI	1.5	0.15	16	~10	~100
16	C	F	H	Cl	OH	MeO	D	C ₁₉ H ₁₈ N ₂ O ₄ ClF·1.0 HCl	0.003	<0.002	1.4	>450	>700
17	C	F	H	Cl	H	MeO	D	C ₁₉ H ₁₈ N ₂ O ₃ ClF·0.34 H ₂ O, 0.95 HCl, 0.08 iPrOH, 0.04 DMF	0.3	0.01	9.3	~30	>900
18	D	F	H	Cl	OH	MeO	D	C ₁₈ H ₁₇ N ₃ O ₄ ClF·1.0 HCl	0.05	0.004	>33	>650	>8000
19	D	F	H	Cl	H	MeO	D	C ₁₈ H ₁₇ N ₃ O ₃ ClF·1.0 HCl	63	1.1	14	~0.2	~13

^a The C,H,N, analysis were obtained for every compounds and were within ±0.4% of the theoretical values unless otherwise stated.

^b Values are averages from at least three independent dose-response curves; variation was generally ±10% for Flt and ±20% for KDR and FTK.

Scheme 1^a

^a (a) SOCl₂/DMF/reflux; (b) iPrOH/reflux.

83. The hydroxybenzophenone **73** was alkylated with 1-bromo-2-methoxyethane under the same conditions used for the nitrophenol derivative **79**. Subsequent nitration of **79** followed by the reduction of the nitro group using iron powder in acetic acid at 100 °C yielded the 2-aminobenzophenone **76**. Diazotation followed by decomposition of the diazonium salt led to the ring closed cinnolinone **82**, which after chlorination using standard conditions (thionyl chloride) gave **83**. Displacement by the appropriate aniline using standard conditions afforded 4-anilinoquinolines **16** and **17** and the 4-anilinoquinazolines **18** and **19**.

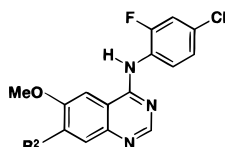
The anilines **86** and **89** were prepared as described in Scheme 8. After protection of the hydroxyl group of the 2-chloro-4-fluorophenol and 4-fluoro-2-methylphenol as methyl carbonates, **84** and **87** were nitrated using nitric acid in sulfuric acid to give the nitro derivatives

85 and **88**. In the case of derivative **85**, the phenol protecting group was cleaved by the conditions used in the work up. The nitro derivatives **85** and **88** were reduced using hydrogenation with iron powder in the presence of iron sulfate or platinum oxide respectively to give the free amines **86** and **89**.

Results and Discussion

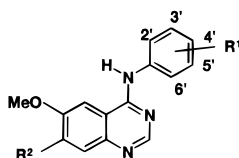
For clarity of discussion, data on only a limited set of compounds are presented in Tables 1–4 and are used to describe the SAR. When trends are exemplified by single pairs of compounds, it is to be understood that more examples^{28,29} have been obtained that support the SAR described below.

Screening of Zeneca's compound collection led to the discovery of a series of C-4 anilinoquinazolines as micromolar inhibitors of the Flt enzyme as illustrated by **2** and **3** (Table 1). Following this discovery, directed robotic synthesis confirmed the potential of this novel series and allowed rapid investigation of aniline ring substitution. From this work and subsequent optimization emerged some general trends: small lipophilic substituents such as halogens or methyl are preferred at the C-4' position of the aniline ring (Table 1, comparison of **2** and **3**, **4** and **8**) (Table 3, comparison of **30**, **34**, and **36**), while small substituents such as fluorine are preferred at the C-2' position (Table 1, **3**, **4**, **6**, and **7**) and hydrogen or small hydrophilic groups

Table 2. Role of the C-7 Side Chain on Enzyme Inhibition

no.	R ²	procedure	formula ^a	enzyme inhibition @ 2 μM ATP concentration IC ₅₀ μM ^b			enzyme selectivity IC ₅₀ ratios	
				Flt	KDR	FTK	FTK/Flt	FTK/KDR
11	MeO(CH ₂) ₂ O	B	see Table 1	0.4	0.007	27	>65	>3800
20	1-pyrrolidinyl-(CH ₂) ₂ O		C ₂₁ H ₂₂ N ₄ O ₂ ClF	0.3	0.04	9.4	>30	>230
21	4-morpholinyl-(CH ₂) ₂ O	B	C ₂₁ H ₂₂ N ₄ O ₃ FCl·2.0 HCl	1.1	0.04	19	>15	>450
22	4-morpholinyl-(CH ₂) ₃ O	B	C ₂₂ H ₂₄ N ₄ O ₃ FCl·1.0 HCl, 0.5 C ₃ H ₆ O ^c	0.2	0.009	6.7	>30	>740
23	4-morpholinyl-(CH ₂) ₄ O		C ₂₃ H ₂₆ ClFN ₄ O ₃ ·1.3 H ₂ O, 1.8 HCl	0.3	0.04	1.5	5	>35
24	4-morpholinyl-(CH ₂) ₂ -O-(CH ₂) ₂ O	E	C ₂₃ H ₂₆ N ₄ O ₄ ClF·1.0 H ₂ O, 1.95 HCl	0.5	0.06	20	40	>330
25	3-thienyl-CH ₂ O	E	C ₂₀ H ₁₅ N ₃ O ₂ ClFS·0.95 HCl	0.8	0.008	>50	>60	>6250
26	4-pyridyl-CH ₂ O	B	C ₂₁ H ₁₆ N ₄ O ₂ ClF·0.5 H ₂ O, 1.95 HCl	1.2	0.06	>33	>25	>550
27	1-imidazolyl-(CH ₂) ₂ O	F	C ₂₀ H ₁₇ N ₅ O ₂ ClF·0.4 H ₂ O, 2.0 HCl	0.1	0.04	2.6	>25	65
28	4-pyridyl-N(Me)-(CH ₂) ₂ O	G	C ₂₃ H ₂₁ N ₅ O ₂ ClF·0.9 H ₂ O, 2.0 HCl	0.1	0.006	1.6	16	>260
29	1-(1,2,4-triazolyl)-(CH ₂) ₂ O	G	C ₁₉ H ₁₆ N ₆ O ₂ ClF·1.6 H ₂ O, 1.0 HCl, 0.35 iPrOH	0.5	0.1	25	50	250
30	1-(1,2,3-triazolyl)-(CH ₂) ₂ O	G	C ₁₉ H ₁₆ ClFN ₆ O ₂ ·1.2 HCl, 0.3 H ₂ O	0.3	0.01	1.8	6	180
31	MeOCH ₂ CONH		C ₁₈ H ₁₆ ClFN ₄ O ₃ ·0.07 HCl, 1.5 H ₂ O	>100	>100	>50		
32	MeN(CH ₂ -CH ₂) ₂ CH-O	H	C ₂₁ H ₂₂ N ₄ O ₂ Cl ₃ ·1.8 HCl, 0.4 H ₂ O	15	1.5	40	~3	~30
33	MeOCH ₂ CONH ^d		C ₁₉ H ₁₉ N ₄ O ₄ F·1.0 HCl, 0.6 H ₂ O	0.3	0.3	>100	>330	>330

^a The C,H,N, analysis were obtained for every compounds and were within ±0.4% of the theoretical values unless otherwise stated. ^b Values are averages from at least three independent dose-response curves; variation was generally ±10% for Flt and ±20% for KDR and FTK. ^c C: calcd, 55.1%; found, 54.7%. ^d 2'-F, 4'-Me, 5'-OH.

Table 3. Role of the Aniline Substituent in the C-7 Triazole-ethoxy Series and HUVEC Activity

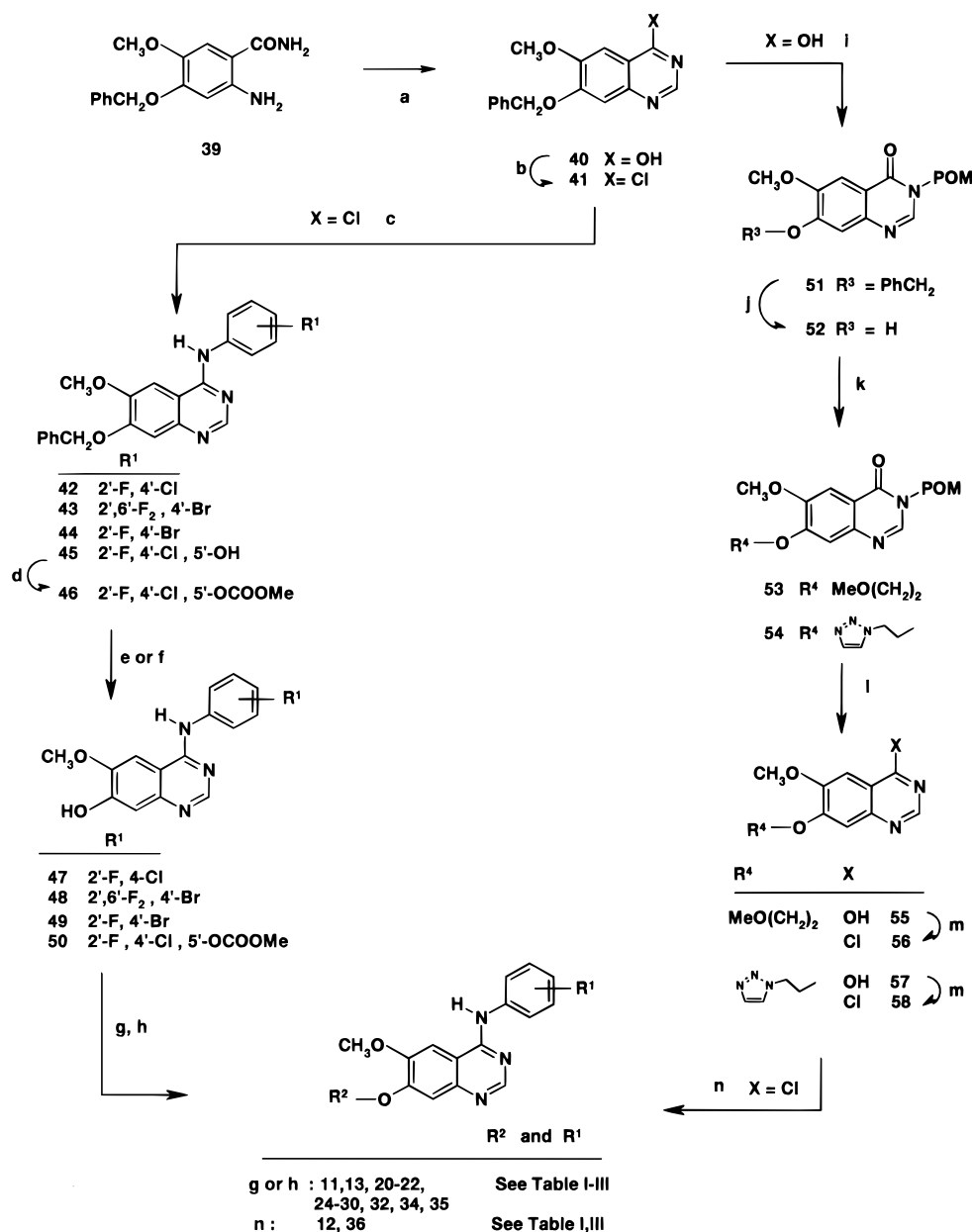
no.	R ¹				R ²	procedure	formula ^a	enzyme inhibition @ 2 μM ATP concentration IC ₅₀ μM ^b			inhibition of HUVEC cell growth IC ₅₀ μM ^c		
	2'	4'	5'	6'				Flt	KDR	FTK	stimulated by		unstimulated
											VEGF	FGF	basal
13	F	Cl	OH	H	MeO(CH ₂) ₂ O		see Table 1	<0.002	<0.002	7.4	0.004	0.8	5
30	F	Cl	H	H	1-(1,2,3-triazolyl)-(CH ₂) ₂ O	G	see Table 2	0.3	0.01	1.8	0.04	1.7	5
34	F	Br	H	H	1-(1,2,3-triazolyl)-(CH ₂) ₂ O	G	C ₁₉ H ₁₆ BrFN ₆ O ₂ ·0.46 H ₂ O, 0.85 HCl	0.7	0.03	>100	0.05	1.5	>10
35	F	Br	H	F	1-(1,2,3-triazolyl)-(CH ₂) ₂ O	E	C ₁₉ H ₁₅ BrF ₂ N ₆ O ₂ ·0.4 H ₂ O, 0.9 HCl	0.8	0.04	6.1	0.02	0.1	1
36	F	CN	H	H	1-(1,2,3-triazolyl)-(CH ₂) ₂ O		C ₂₀ H ₁₆ FN ₇ O ₂ ·1.25 HCl, 0.3 H ₂ O	8.1	0.3	45	0.6	3	>10

^a The C,H,N, analysis were obtained for every compounds and were within ±0.4% of the theoretical values unless otherwise stated. ^b Values are averages from at least three independent dose-response curves; variation was generally ±10% for Flt and ±20% for KDR and FTK. ^c Values are averages from at least three independent dose-response curves; variation was generally ±15% for VEGF and FGF.

are best at the meta positions (C3' or C5') (Table 1, comparison of **3–5**, **8**, **9**, and **10**). From this screening, it also became apparent that a meta-hydroxy substituent produced increased potency (~180-fold) particularly against Flt (Table 1, comparison of **2** and **5**, **4** and **10**, and **11** and **13**). This effect suggests a possible additional interaction with the enzyme and will be discussed latter in the modeling section.

Investigation of the C-6 and C-7 positions of the quinazolinone nucleus indicated that, in general, a small-electron-donating substituent at C-6 such as methoxy

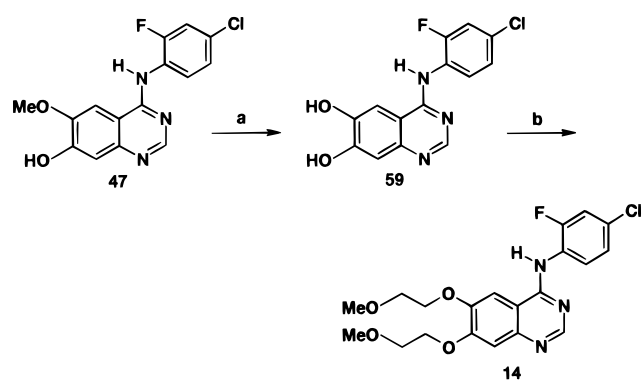
is well-tolerated and preferred to hydrogen or more bulky substituents as illustrated by the comparison of **11**, **14**, and **15** (Table 1). A C-6 hydrogen led to a ~20-fold reduction in KDR potency, while introduction of a bulky, flexible methoxyethoxy side chain led to a ~10-fold drop in KDR inhibition. In contrast to the C-6 position, a large range of substituents differing in their lipophilic, basic, electronic and steric nature were tolerated at C-7 of the quinazolinone ring (Table 1 and 2). Replacement of the C-7 methoxy by a longer methoxyethoxy side chain led to 5- to >10-fold increases in Flt

Scheme 2^a

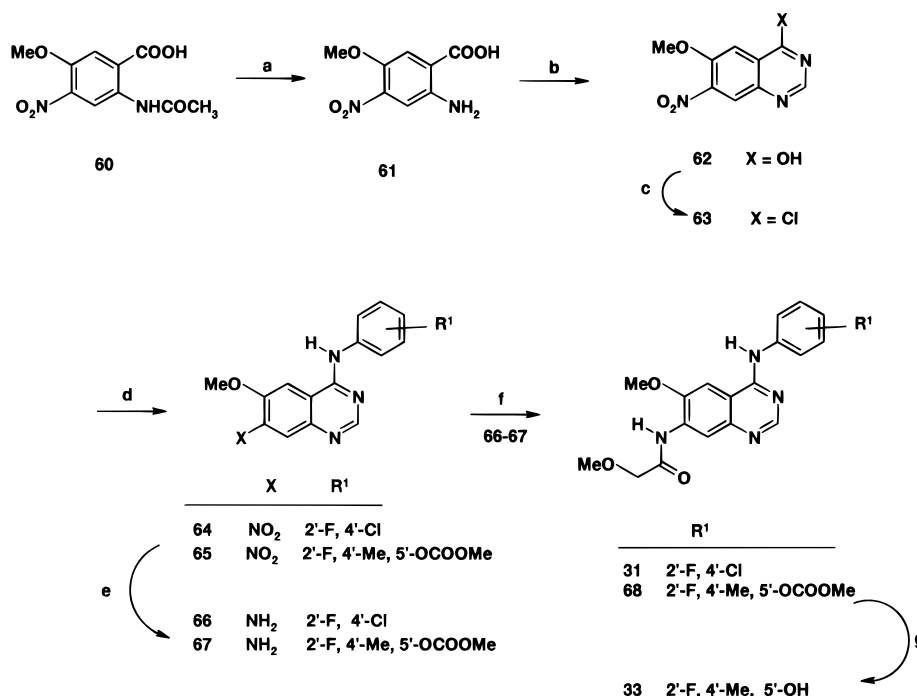
^a (a) Gold's reagent/dioxane/reflux; (b) SOCl₂/DMF/reflux; (c) ArNH₂/iPrOH or 2-pentanol/reflux; (d) Et₃N/(CH₃CO)₂O/CH₂Cl₂; (e) TFA/reflux; (f) H₂/10% Pd/C; (g) R²X/K₂CO₃/DMF/60 °C; (h) R²OH/DEAD/Ph₃P/CH₂Cl₂ or R²OH/ADDP/nBu₃P/CH₂Cl₂; (i) (1) NaH/DMF, (2) tBuOCOCl; (j) H₂/10% Pd/C/CH₃COOH; (k) MeO(CH₂)₂OH or 1-(1,2,3-triazolyl)-(CH₂)₂OH/Ph₃P/DEAD/CH₂Cl₂; (l) NH₃/MeOH; (m) SOCl₂/DMF/reflux; (n) ArNH₂/iPrOH/reflux.

and KDR enzyme inhibition as indicated by the comparison of **4** and **11**, **5**, and **12** (Table 1). A similar improvement in enzyme inhibition was observed in the C-7 morpholinoalkoxy series where the propoxy side chain gave better potency than ethoxy or butoxy linkers (**21–24**) (Table 2). Introduction of basic and/or heteroaromatic substituents such as imidazole, triazole, or ethoxy-aminopyridine led to very potent submicromolar inhibitors of both VEGF RTK enzymes (**25–30**) (Table 2).²⁹ The ability of the C-7 position of the quinazoline to accept a large diversity of substituents suggests that this extremity of the molecule probably points toward the solvent (see modeling section).

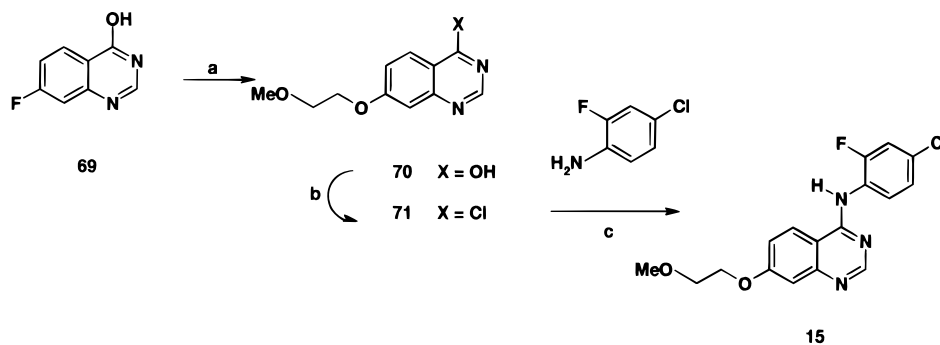
In contrast, the introduction of substituents possessing reduced flexibility at C-7 was less well tolerated in the 2-fluoro-4-chloro series and led to compounds show-

Scheme 3^a

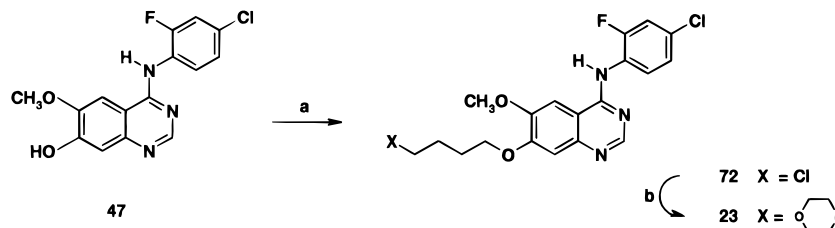
^a (a) C₆H₅N/HCl; (b) bromoethyl methyl ether/K₂CO₃/DMF.

Scheme 4^a

^a (a) HCl/reflux; (b) HCONH₂/reflux; (c) SOCl₂/DMF/reflux; (d) R¹ArNH₂/iPrOH/reflux; (e) H₂/10% Pd/C/MeOH/DMF or EtOH; (f) CH₃OCH₂COCl/CH₂Cl₂/pyridine; (g) NaOH/MeOH/0 °C.

Scheme 5^a

^a (a) (1) Na/CH₃O(CH₂)₂OH, (2) reflux; (b) SOCl₂/DMF/reflux; (c) iPrOH/reflux.

Scheme 6^a

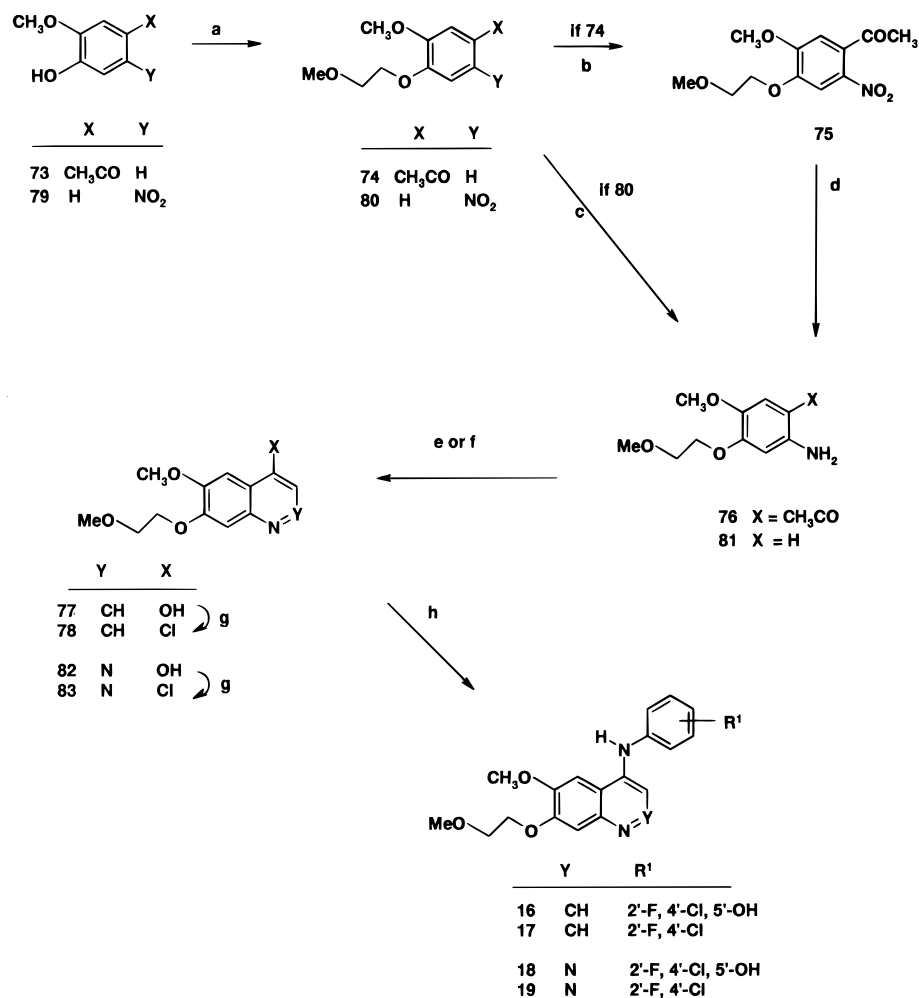
^a (a) Cl(CH₂)₄Br/K₂CO₃/DMF/40 °C; (b) morpholine/110 °C.

ing reduced enzyme inhibitory properties (comparison of **11** with **31–32**) (Table 2). However, despite the reduced flexibility, good potency can be retained in the meta-hydroxy subseries with the C-7 amide side chains as illustrated by the comparison of **31** and **33** (Table 2), suggesting that the putative interaction of the meta-hydroxyl with the protein is strong enough to compensate in part for the C-7 constraints.

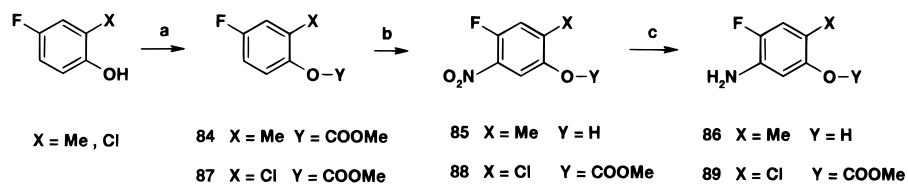
Combination of some of the best substituents on the aniline ring (e.g., 2-fluoro-4-chloro or 2-fluoro-4-methyl-

5-hydroxy) and at the C-6 and C-7 positions of the quinazolinone nucleus led to nanomolar inhibitors of the Flt and KDR enzymes as illustrated by **10** and **13** (Table 1).

Replacement of the quinazolinone nucleus was also investigated. Heteroaromatic bicycles such as quinoline or cinnoline (series C and D in Table 1) produced notable effects. In the 2-fluoro-4-chloroanilino series, the quinoline derivative is almost equipotent to the quinazolinone (comparison **11** and **17**, Table 1). Replacement by a

Scheme 7^a

^a (a) Bromoethyl methyl ether/K₂CO₃/DMP; (b) HNO₃/2 °C; (c) H₂/10% Pd/C/EtOAc; (d) Fe/CH₃COOH/100 °C; (e) **76**: NaNO₂/H₂SO₄/CH₃COOH/80 °C; (f) **81**: (1) diethyl ethoxymethylenemalonate/110 °C, (2) PhOPh/240 °C; (g) SOCl₂/DMF/reflux; (h) ArNH₂/DMF/150 °C.

Scheme 8^a

^a (a) Methyl chloroformate/NaOH; (b) H₂SO₄/HNO₃; (c) **88**: PtO₂/EtOH, **85**: iron powder/FeSO₄.

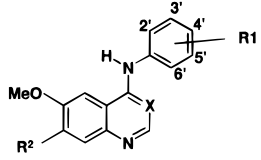
cinnoline nucleus is tolerated but led to ~160-fold reduction in potency (comparison **11** and **19**, Table 1). The favorable effect of the meta-hydroxy substituent observed in the anilinoquinazoline series is also present in the quinoline series (~100-fold), leading to nanomolar inhibitors of both VEGF enzymes (comparison of **16** and **17**, Table 1). This meta-hydroxy substitution also confers submicromolar level of potency in the cinnoline series (comparison **18** and **19**, Table 1).

In an attempt to gain insight into the structural basis of the inhibitory activity of our series, we have developed a binding model to the enzyme that is consistent with the SAR data. This model is discussed in the modeling section below.

Enzyme and Cell Selectivity. Selectivity was measured against FGFR-1 (FTK) another important RTK thought to be important in angiogenesis.

As shown by **5**, **10**, and **11–14**, compounds from both the 2-fluoro-4-chloro and 3-hydroxy anilinoquinazoline series are very selective inhibitors of the VEGF RTKs, Flt, and KDR, compared to the FGF RTK with ratios of IC₅₀s ranging respectively from 50- to >3800-fold (Table 1). C-7 side chain modifications were also useful to improve the selectivity (comparison of **4** and **11**, **21**, **22**, **25**, **26**) (Table 1 and 2). Similarly, the quinoline and cinnoline series provided very selective VEGF RTK inhibitors as illustrated by KDR/FTK potency ratios ranging from ~30 to >8000-fold (**16–18**, Table 1).

Interestingly, although the anilinoquinazoline series had previously delivered potent EGF RTK inhibitors,^{30–33} we found that distinct SAR existed for EGF RTK and VEGF RTK inhibitions. On the aniline ring, the EGF preferred substitution, namely, a lipophile (Cl, Br, ...) ^{25,30–33} at the C-3' position is not optimal for VEGF

Table 4. Mouse Plasma Levels Following Oral Administration of 100 mg/kg of Compound


no.	X	R ¹			R ²	plasma level μM^a	
		2'	4'	5'		@ 6 h	@ 24 h
4	N	F	Cl	H	MeO	NT ^b	NT ^b
10	N	F	Cl	OH	MeO	<0.2	<0.2
11	N	F	Cl	H	MeO(CH ₂) ₂ O	12	<0.1
12	N	H	H	OH	MeO(CH ₂) ₂ O	NT ^b	NT ^b
13	N	F	Cl	OH	MeO(CH ₂) ₂ O	<0.1	<0.1
17	CH	F	Cl	H	MeO(CH ₂) ₂ O	3	NT ^b
22	N	F	Cl	H	4-morpholinyl-(CH ₂) ₃ O	4	0.8
24	N	F	Cl	H	4-morpholinyl-(CH ₂) ₂ -O-(CH ₂) ₂ O	11	<0.1
27	N	F	Cl	H	1-imidazolyl-(CH ₂) ₂ O	11	<0.1
30	N	F	Cl	H	1-(1,2,3-triazolyl)-(CH ₂) ₂ O	49	10
34	N	F	Br	H	1-(1,2,3-triazolyl)-(CH ₂) ₂ O	45	13

^a Variation was generally $\pm 15\%$. ^b NT: Not tested.

inhibition (**4**, **8**, and **9**, Table 1). In addition, it is noteworthy that compound **9**, a well-known extremely potent inhibitor of EGF RTK (IC_{50} : 9 nM)³³ is a 100–10000 times less active as an inhibitor of Flt and KDR (Table 1). Furthermore, **9** is >50-fold less active against Flt than its isomer **4**, which possesses one of the preferred substitutions (2-fluoro-4-chloro) for inhibition of VEGF RTKs. Similarly, the EGF preferred quinazoline substitution, namely, a large C-6 substituent^{25,28,30,31,34} is not optimal for potent inhibition of the Flt and KDR enzymes (**11** and **14**).

Molecular Modeling: Development of a Binding Model for the Anilino-quinazoline, -quinoline, and -cinnoline Series. Our study relies on the key structure–activity relationships described in this paper and on the published structural data on the protein kinase family (see Experimental Section).

Recently, an increasing number of 3D structures of protein kinases, especially kinases bound to diverse competitive inhibitors, have been published, improving our knowledge of the key hydrogen bond interactions with the enzyme backbone and of the role of the conserved residues clustered near the active site.^{35–47} The adenine moiety of ATP is anchored in the active site by two hydrogen bonds, one donating and one accepting. As illustrated in Figure 2, one involves the N-6 hydrogen (donating) and the backbone carbonyl of Glu-121, the other involves the N-1 of adenine (accepting) and the backbone amide of Val-123. Most of the experimental or modeled enzyme–inhibitor complexes show a similar hydrogen bond pattern.^{36,39,44,48–51} In other complexes,^{36,43,45} the accepting hydrogen bond is conserved, whereas the donating hydrogen bond is now closer to the entry of the active site and shared with the backbone carbonyl of the residue equivalent to Val-123 (Figure 2). In a few other cases,^{40,46,47} the inhibitors are anchored in the adenine site only by the highly conserved, accepting hydrogen bond interaction. Although the H-bonding is essential for inhibitor binding, the number of protein–ligand hydrogen bonds is not correlated to potency. Modeling^{48,50–52} and experimental^{45–47} studies have also revealed the presence of a deep, medium size, pocket adjacent to the adenine binding

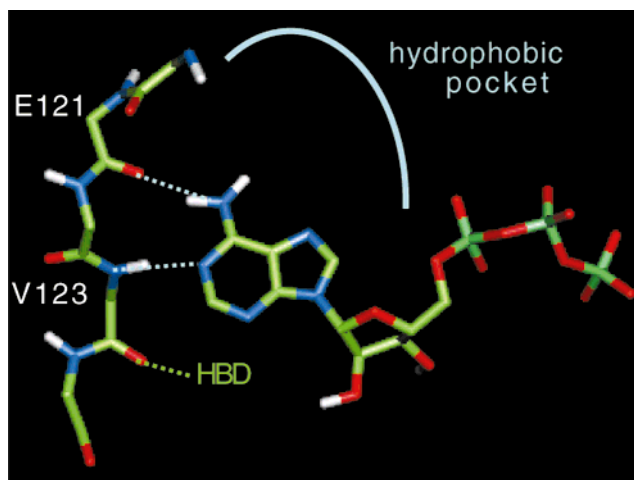


Figure 2. Schematic representation of ATP bound to the PKA active site.⁵³ The adenine moiety is anchored by one donating and one accepting H-bond (blue dotted lines). Other kinase-inhibitor complexes^{36,43,45} have shown that another H-bond could be formed between an H-bond donor (HBD) and the backbone carbonyl of residue equivalent to Val-123 (green dotted line). The location of the hydrophobic pocket is also shown.

site. This hydrophobic pocket, made up of conserved and nonconserved residues, is not utilized by the ATP itself, but can be exploited by inhibitors from various chemical classes. It is now evident that potency and partial selectivity can be achieved by small molecule inhibitors that occupy this pocket.

The full enzyme kinetic profile of our series of VEGF RTK inhibitors has not been measured. However, results from experiments varying ATP concentration in the kinase assays are consistent with ATP competition.²⁸ Furthermore, it has been shown that the potent EGF–RTK inhibitor *N*-(3-chlorophenyl)-4-quinazolinylamine is competitive with respect to ATP,³⁰ strongly suggesting to us that our compounds inhibit the catalytic activity of Flt and KDR through a similar process. Therefore, using a 3D homology model of Flt1 based on the X-ray structure of PKA,⁵³ we have searched for a binding mode that would fit our compounds into the ATP binding site and be consistent with the SAR data.

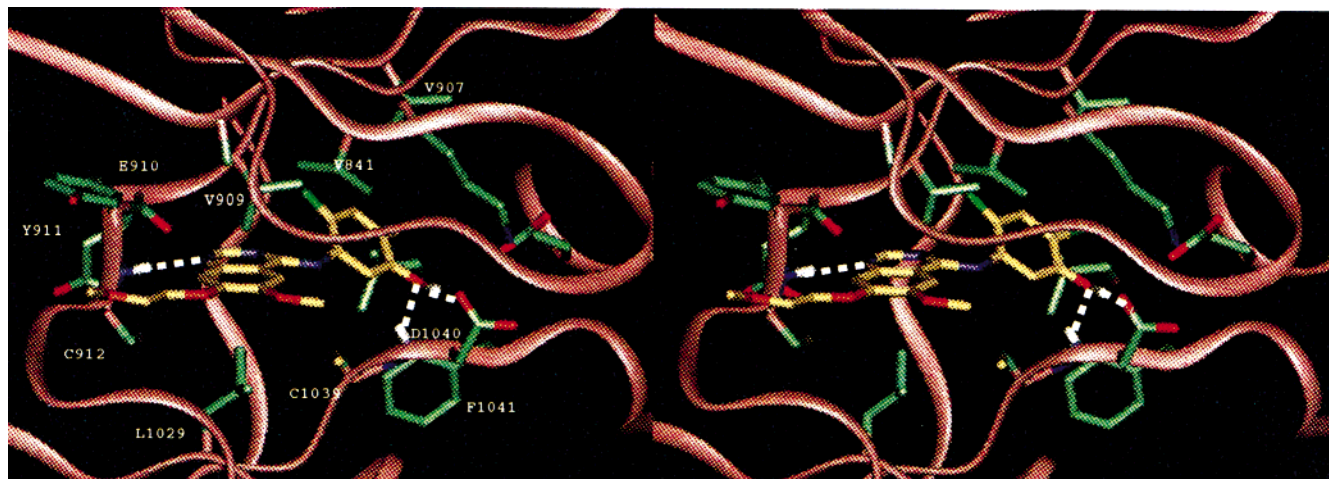


Figure 3. Stereoview of compound **13** docked into the ATP-binding site of the homology model of Flt-1. Hydrogen bond interactions are represented as dotted lines. To remain consistent with other published models, residues are numbered as in the complete sequence of Flt-1. The quinazoline ring occupies the adenine binding site, and the anilino moiety is buried into the deep hydrophobic pocket. The C-6 and C-7 side chains are oriented toward the entrance of the binding site and extend out of the pocket. The N-1 of the quinazoline nucleus forms an H-bond with the backbone NH of Cys-912 (residue homologue to Val-123 in PKA). A second H-bond may be formed between the hydroxyl group of the phenol moiety and the carboxylic function of Asp-1040 (residue equivalent to Phe-185 in PKA). In that position, the phenolic oxygen could also interact with the backbone NH of Asp-1040. Some of the residues that make hydrophobic contacts with the inhibitor are also shown.

The binding mode that was most satisfactory is illustrated in Figure 3 for the quinazoline derivative **13**. In this model, the quinazoline ring occupies the flat and rather narrow adenine site. The highly conserved accepting hydrogen bond is realized by N-1 of the quinazoline, which binds to the backbone amide of Cys-912 (equivalent to Val-123 in PKA), whereas N-3 does not participate in any hydrogen bonding. The C-2 of the quinazoline is located close to the carbonyl oxygen of Glu-910. This binding mode possibly explains the relatively lower potency observed in the cinnoline series, where C-2 is replaced by nitrogen (**11**, **19**) (Table 1), leading to unfavorable repulsive electrostatic interactions. It also possibly explains the equipotency observed between the quinazoline and the quinoline series (**11**, **17**) (Table 1), as the quinazoline N-3, which is in van der Waals contacts with Val-909, can be replaced by a carbon atom in the quinoline.

In our model (see Experimental Section), the 2-fluoro-4-chloro anilino substituent is buried in the hydrophobic pocket adjacent to the adenine site. The limited size of this pocket explains the rather limited substitution pattern allowed on the phenyl ring. The C-6 and C-7 side chains are then oriented completely opposite, toward the outside of the cleft. This is consistent with the rather broad substitution pattern on C-7, but not the more restricted substitution observed for the C-6 position. This underlines the limits of the homology model; prediction is less accurate when moving away from the highly conserved binding site.

The ~180-fold increase in potency observed in the meta-hydroxy anilinoquinazoline, quinoline, and cinnoline derivatives (**12**, **13**, **16**, **18**) (Table 1) suggests the existence of an extra interaction with the enzyme. In the binding mode we propose, this hydroxy group forms a hydrogen bond with the flexible side chain of Asp-1040, a residue of the highly conserved segment -Asp-Phe-Gly, which normally participates in MgATP coordination. In this position, the phenolic oxygen could also interact with the backbone NH of Asp-1040. The sub-

micromolar level of potency in the otherwise moderately active cinnoline series suggests that this interaction slightly reorients the molecule in the active site so that the repulsive electrostatic interactions with Cys-912 does not occur or is significantly reduced. The beneficial effect of an hydroxy in an analogous position has also been observed in a series of pyrazolopyrimidine, inhibitors of EGF RTK.⁵⁰ In their model, the authors assume that the phenol moiety occupies the deep hydrophobic pocket and suggest the existence of an hydrogen bond between the hydroxyl group and the backbone of Phe-832 (in their EGF RTK model, equivalent to Phe1041 in our Flt1 model). An analogous hydrogen bond has also been experimentally identified in the complex of FGFR1 with PD173074,⁴⁵ a pyrido[2,3-*d*]pyrimidine derivative; while the 6-(3,5-dimethoxy)-phenyl substituent is buried in the hydrophobic pocket, one of the methoxy oxygens interacts with the amide nitrogen of Asp-641 (Asp-1040 in Flt1). Interestingly, minimal or more pronounced shifts in the backbone and side chains of these conserved Asp and Phe has been observed upon inhibitor binding.^{35,38,39,41} All these observations suggested that depending on the chemical class of inhibitor, the molecular model used and on the kinase in question, different hydrogen bonds can be formed with this Asp-Phe segment. However, while it is reasonable to assume that this segment can provide strong hydrogen bond interactions with inhibitors it remains difficult to define its exact location, as the molecular modeling technique is fairly limited in predicting conformational changes or more subtle adjustment of specific residue positions upon inhibitor binding.

Cellular Activity. Our most potent and selective kinase inhibitors were evaluated for their ability to inhibit the incorporation of tritiated thymidine during the growth of human umbilical vein endothelial cells (HUVECs) stimulated by VEGF *in vitro*. As shown in Table 3, the potency observed against the one or more isolated enzymes translated to a submicromolar level of inhibition of stimulated cell growth. Moreover, an

Table 5. Inhibition of Rat Uterus Weight Gain Following Administration of VTK Inhibitors

no.	dose (mg/kg) @ -18 and -1 h	% inhibition of uterus weight gain	significance (p)
4	100	34	<0.05
10	60	80	<0.05
11	100	31	<0.05
12	100	NA ^a	
22	100	59	<0.05
34	NT ^b		

^a NA: not active. ^b NT: not tested.

excellent level of selectivity is conserved in cells as indicated by the 5- to ~200-fold selectivity ratios observed between the inhibition of VEGF and FGF stimulated HUVEC growth (**13**, **30**, **34**) (Table 3). The slight reduction in selectivity observed between enzyme and cell data may be explained by differences in ATP concentrations between the enzyme assay and whole cells. Interestingly, inhibition of KDR RTK alone appeared to be sufficient to provide inhibition of VEGF signaling in HUVECs (**34**, **35**, **36**) (Table 3). The 50- to 1250-fold higher concentrations needed to inhibit the growth of unstimulated HUVECs (basal IC₅₀) compared to those required for the inhibition of VEGF stimulated HUVECs growth indicates that these compounds do not impart any direct cytostatic or cytotoxic effect (Table 3).

Plasma Levels in Mice. As shown in Table 4, the 2-fluoro-4-chloro-anilinoquinazolines listed are bioavailable orally when dosed to mice at 100 mg/kg and achieved good total plasma levels as illustrated by the concentrations obtained at 6 h. Comparison of plasma levels of quinazoline derivative **11** and quinoline **17** indicates a clear difference in this species between the two series, the latter showing lower plasma levels in mice, which may be a consequence of a higher degree of metabolism.²⁸ In contrast to the 2-fluoro-4-chloro-anilino series, in mice, the meta-hydroxy anilinoquinazoline series plasma levels (**13**) were below the limit of detection at 6 h. Evaluation of the plasma levels following oral dosing in rat of key representatives of the meta-hydroxy series showed a similar pattern. In some cases, the glucuronide of the phenol moiety was detected suggesting a very high degree of conjugation of this meta-hydroxy subseries.

Heteroaromatic C-7 side chains such as imidazole and triazole led to high-plasma levels as shown respectively by **27** and **30**, **34**. In these latter cases, total plasma levels are maintained above 10 μM for as long as 24 h (Table 4).

Activity in Vivo. In immature rats, the initial increase in uterine weight observed following administration of estradiol is primarily due to tissue oedema induced by expression of VEGF in the uterus. A VEGF sequestering agent (VEGF m-Ab, 100 μg/rat) administered intraperitoneally 18 h prior to estradiol treatment inhibit this early uterotrophic effect by up to ~80%. The test used to evaluate our inhibitors measured their capacity to reduce the acute increase in uterine weight at 5 h following oestrogen stimulation.

As shown in Table 5, when administered orally at a dose of 100 mg/kg at 18 h and 1 h prior to estradiol injection, the 2-fluoro-4-chloro anilinoquinazoline series significantly inhibited the increase in weight of the rat

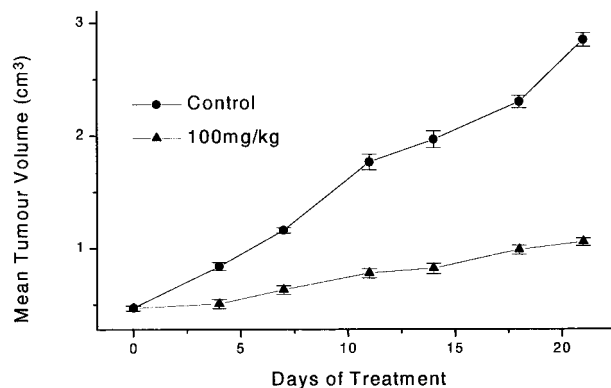


Figure 4. Growth inhibition of established Calu-6 tumor xenografts treated with **34**. Nude mice bearing Calu-6 xenografts received a daily oral dose of vehicle (●) or 100 mg/kg **34** (▲). Data points represent the mean (±SEM) of 10 (control) and 9 (treated) mice respectively.

uterus. Up to 59% inhibition was obtained with **22**. The most profound effect was observed with the most potent kinase inhibitor from the meta-hydroxy series **10**, which exhibited ~80% inhibition with two doses of 60 mg/kg. This was surprising given its plasma pharmacokinetic profile in mice (Table 5) and suggested that the pharmacokinetics of such compounds may be different in rat. In this latter species, following oral dosing (100 mg/kg), **10** showed low but detectable 6 h plasma levels (~1 μM), which in this acute model and due to the excellent intrinsic potency of this molecule is probably sufficient to explain the level of efficacy observed. Because of the PK differences observed between rat and mouse as well as the acute effect seen in this test, the rat uterine oedema assay was used as a measure of VEGF pharmacology but appeared not as discriminatory to predict efficacy in chronic models such as xenografts.

VEGF RTK inhibitors were also evaluated for their ability to inhibit growth of human tumors implanted subcutaneously in athymic mice. Oral administration of **34** (100 mg/kg/day) for 21 days to mice with established Calu-6 lung carcinoma (0.5 cm³) xenografts markedly inhibited tumor growth by 75% (p < 0.001, one tailed t-test) (Figure 4), without causing any loss of animal condition. It is noteworthy that **34** does not inhibit the in vitro growth of Calu-6 cells (IC₅₀ > 70 μM) at levels of compounds likely to be freely available in vivo (Mouse SPB: 98% ± 0.5%)(mean ± SE, n = 5), which indicates that even taking into account a likely accumulation of the compound, the tumor growth inhibition observed cannot be attributed to a direct cytotoxic or cytostatic effect on tumor cells.

Comparable efficacy has since been confirmed on other human tumor xenografts including colon, lung, breast, prostate, and ovary tumors.⁵⁴

Conclusions

Novel anilinoquinazolines carrying small lipophilic 2' and 4' substituents, a C-6 methoxy, and a wide range of C-7 substituents are nanomolar inhibitors of the VEGF receptor tyrosine kinase enzymes. Addition of a meta-hydroxy group on the aniline nucleus enhances the potency of this series of molecules.

Using a molecular model of VEGF RTK, Flt-1, a possible binding mode for this series of inhibitors has

been identified that is consistent with the observed SAR and published structural data on kinase-inhibitor complexes.

Most of these derivatives are potent submicromolar inhibitors of human endothelial cell proliferation stimulated by VEGF. The anilinoquinazolines and quinolines are highly selective inhibitors of Flt and KDR tyrosine kinase (up to >1000-fold), in comparison to FGF RTK and this enzyme selectivity profile translates well into cell selectivity.

Many of the anilinoquinazolines are orally absorbed in rats and mice and are effective in inhibiting the acute, VEGF-mediated, uterotrophic response to estradiol in rats, and the growth of human xenograft tumors in athymic mice. The anilinoquinolines are less effective *in vivo* probably because of rapid metabolism.

The anilinoquinazoline **34** (ZD4190) was identified as one of the most promising representatives of this new series of molecules. In view of its biological properties and efficacy *in vivo*, this compound was selected for development and is currently undergoing preclinical studies to further define its efficacy and toxicology profile.

Experimental Section

Protein Modeling. The first 3D crystal structure of the catalytic domain of a protein kinase to become available was that of the cAMP-dependent protein kinase A, PKA.⁵³ The crystal structure revealed a bilobal shape, with a large cleft separating the two lobes and providing the binding site for ATP. The adenine ring is buried in the hydrophobic bottom of the cleft, while the sugar and triphosphate moieties extend toward the opening of the cleft. This typical architecture was evident in subsequent crystal structures,^{55–58} indicating a conserved ATP binding mode, in agreement with the high degree of sequence similarity displayed by the kinase catalytic core.⁵⁹ However, the structure of the ternary complex PKA–ATP–PKI⁵² was, for a while, the only kinase structure available in its active closed form;⁶⁰ therefore, it has been extensively used as the reference for homology modeling of other members of the protein kinase family. These models have been successfully utilized to understand SAR data and guide medicinal chemistry programs.^{48–52,61}

The 3D model of human VEGF RTK, Flt-1, was built with the automated homology modeling program Modeler⁶² interfaced with the molecular modeling software Quanta.⁶³ The crystal structure of the ternary complex of PKA (PDB entry 1ATP) was used as a template.⁵³ The basis for the 3D model was the sequence alignment with the kinase family; all the key and conserved residues have been aligned and most of the deletions or insertions have been assigned using the published multiple sequence alignment of kinases.⁵⁹ However, Flt-1 has two large insertions, one near the beginning of the C-terminal domain (Asp926–Glu992), the other in the C-terminal tail (Phe1182–Leu1232). As it is reasonable to think that they are not part of the active site and as they are too large to be modeled, we have removed them from the original sequence.

In the PKA structure, the nonconserved carboxy-terminal tail extends over the surface from the large lobe to the top of the small lobe. In the closed ternary complex, residue Phe327 of the C-terminal TSNFDDY motif makes part of the adenosine binding pocket. Experimental data have shown that Phe327 is expelled from its position upon binding of the inhibitor staurosporine.⁴¹ In the open binary complex PKA–PKI, the C-terminal segment, and Phe327 in particular, undergoes an even larger shift, leaving the adenosine site more accessible to the solvent.⁶⁰ Intriguingly, Flt-1 has a similar TSMFDDY sequence in its carboxy-terminal tail, whereas KDR itself, which has 70% sequence similarity over the kinase domain with Flt-1, does not have this motif. Moreover, none of the

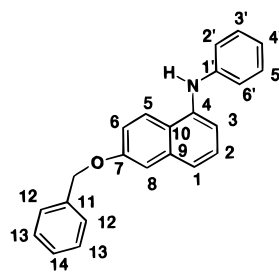


Figure 5.

other known human PTKs have this motif. Therefore, it is not clear whether this similarity is fortuitous or not and we do not know if this segment occupies a similar location to that observed in the 3D structure of PKA. In Flt-1, the presence of a large insertion preceding this segment could modify its position. The C-terminal sequence has been, however, included in our original homology model of Flt-1. When docking our inhibitors, it is obvious that steric clashes occur between the C7-side chains and the Phe1039 (equivalent to Phe327 in PKA). This suggested to us that either the 3D location of this segment is wrong or this segment is subject to large conformational changes as experimentally observed in PKA.^{41,60} Therefore, we have truncated the model for our subsequent docking studies. Before that, a final check and a geometry optimization of the amino acids chains lying within the active site was performed, using the CHARMM force field^{64,65} implemented in Quanta 97.⁶³ The VEGF RTK inhibitors were built in Quanta and the charges were assigned by the Quanta charge template method.⁶³ These inhibitors have been docked manually into the ATP binding site, and the amino acid side chains were reoriented when unfavorable steric interactions occurred. The most relevant solutions were then energy minimized with the CHARMM force field to relieve remaining unfavorable steric contacts.

Very recently, the structure of the kinase domain of human KDR has been published⁶⁶ (PDB entry 1VR2). The authors have compared the ATP binding site of KDR and FGFR1 and came to the conclusion that the overall architecture of the site is conserved. As the coordinates of KDR are not yet available, we have checked our binding mode by docking our compounds into the ATP binding site of the FGFR1 structure (PDB entry 1FGK).³⁶ All the key interactions we have described previously are conserved, which justify the use of PKA as a template for our homology model of Flt-1.

General Procedures. All experiments were carried out under an inert atmosphere and at room temperature unless otherwise stated. Flash chromatography was carried out on Merck Kieselgel 60 (Art. 9385). The purities of compounds for test were assessed by analytical HPLC on a Hichrom S50DS1 Spherisorb Column System set to run isocratically with 60–70% MeOH + 0.2% CF₃COOH in H₂O as eluent. TLCs were performed on precoated silica gel plates (Merck Art. 5715), and the resulting chromatograms were visualized under UV light at 254 nm. Melting points were determined on a Kofler Block or with a Büchi melting point apparatus on compounds isolated as described in the experimental procedures and are uncorrected. The NMR spectra were determined in Me₂SO-*d*₆ solution (unless otherwise stated) on a Bruker AM 200 (200 MHz) spectrometer or on a JEOL JNM EX 400 (400 MHz). For the ¹³C NMR spectra, ring carbon atoms have been numbered as shown below. For ¹H NMR spectra, hydrogens have been given the numbering of the carbon atom they are attached to (Figure 5).

Chemical shifts are expressed in unit of δ (ppm), and peak multiplicities are expressed as follows: s, singlet; d, doublet; dd, doublet of doublet; t, triplet; br s, broad singlet; m, multiplet. Fast atom bombardment (FAB) mass spectra were determined with a VG MS9 spectrometer and Finnigan IncoS data system, using Me₂SO as the solvent and glycerol as the matrix or with a Finnigan SSQ 7000 for the electro-spray technique. With the appropriate mode, either positive or

negative ion data could be collected. NMR and mass spectra were run on isolated intermediates and final products and are consistent with the proposed structures. For the microanalysis, all the adducts mentioned were measured: water was measured by the Karl-Fisher method using a Mettler DL 18; HCl content was determined by titration using silver nitrate solution and a Metrohm 686 and the organic adducts were measured by ^1H NMR.

The anilines used (2-fluoro-4-chloro; 4-chloro; 2-fluoro; 4-chloro; 3-hydroxy; 2-chloro-4-iodo; 2,4-difluoro; 3-chloro-4-fluoro; 2,4-difluoro; 3-chloro-4-fluoro; 2-fluoro-4-bromo; 2,6-difluoro-4-bromo) were commercially available. 4-(2-Chloroethyl)morpholine hydrochloride, 1-(2-chloroethyl)pyrrolidine hydrochloride, 3-thiophenemethanol and 4-(chloromethyl)pyridine hydrochloride were purchased from Aldrich. The 4-(3-chloropropyl)morpholine was prepared as described in ref 67.

The following abbreviations have been used: DMF: *N,N*-dimethylformamide; DEAD: diethylazodicarboxylate; ADDP: 1,1'-(azodicarbonyl)dipiperidine; Gold's reagent: [3-(dimethylamino)-2-azaprop-2-en-1-ylidene]dimethylammonium chloride; TFA: trifluoroacetic acid; DMSO: dimethyl sulfoxide.

The anilinoquinazolines **2–10** were prepared by multiparallel synthesis. Eight reactions were conducted in parallel in 10 mL tubes. The tubes were heated in a 10 holes heater. The experimental details of this reaction are described below for the preparation of compound **2**.

***N*-(2-Fluorophenyl)-6,7-dimethoxy-4-quinazolinyllamine 2. (Procedure A).** To a mixture of 2-fluoroaniline (136 mg, 1.22 mmol) in 2-propanol (6 mL) was added 5.5 N hydrogen chloride in 2-propanol (0.22 mL) followed by 4-chloro-6,7-dimethoxyquinazoline **38**²⁵ (247 mg, 1.1 mmol). After heating at 80 °C for 4 h, the mixture was cooled and ether (5 mL) was added. The solid was filtered, washed with ether (2 × 5 mL), and dried under vacuum overnight at 50 °C to give 338 mg of **2** (91%). ^1H NMR: δ 4.05 (s, 6H, 2 CH₃O), 7.3–7.5 (m, 3H, H3', H4' and H5'), 7.4 (s, 1H, H8), 7.6 (t, 1H, H6'), 8.3 (s, 1H, H5), 8.8 (s, 1H, H2). ^{13}C NMR: δ 56.5 (O–CH₃), 56.9 (O–CH₃), 99.6 (C8), 104.0 (C5), 106.9 (C10), 116.3 (d, C3', J C–F = 19.6 Hz), 124.4 (d, C1', J C–F = 7.7 Hz), 124.8 (C5' or C4'), 128.8 (C4' or C5'), 129.2 (d, C6', J C–F = 7.7 Hz), 135.4 (C4), 148.7 (C2), 150.3 (C9), 156.5 (C7), 156.9 (d, C2', J C–F = 249.1 Hz), 159.1 (C6). MS–ESI *m/z* 300 [MH]⁺. Anal. (C₁₆H₁₄O₂N₃F·1.1 HCl, 0.1 H₂O) C, H, N.

A similar procedure was used to prepare **3–10**, **12**, **64**, and **65**. In the case of **64** and **65**, the corresponding chloroquinazoline hydrochloride was used and the reaction was carried out without addition of hydrogen chloride in 2-propanol.

***N*-(4-Chloro-2-fluorophenyl)-6-methoxy-7-(2-methoxyethoxy)-4-quinazolinyllamine hydrochloride 11. (Procedure B).** 2-Bromoethyl-methyl ether (712 μL , 7.56 mmol) was added dropwise to a solution of *N*-(4-chloro-2-fluorophenyl)-7-hydroxy-6-methoxy-4-quinazolinyllamine **47** (2.2 g, 6.88 mmol) and potassium carbonate (2.84 g, 20.6 mmol) in DMF (110 mL). The mixture was stirred for 10 h at 60 °C, then for 2 days at ambient temperature. The solvent was removed by evaporation, and the crude product purified by flash chromatography eluting with ethyl acetate/petroleum ether (4:1). The resulting solid was dissolved in hot ethanol and 3 N hydrogen chloride in ethanol was added. After cooling, the resulting solid was collected by filtration, washed with ethanol, and dried under vacuum to give 1.74 g of **11** (62%). Mp 255–257 °C. ^1H NMR (DMSO-*d*₆; CD₃COOD): δ 3.36 (s, 3H, CH₃O), 3.79 (t, 2H, CH₂O), 4.02 (s, 3H, CH₃O), 4.34 (t, 2H, CH₂O), 7.33 (s, 1H, H8), 7.46 (dd, 1H, H3'), 7.60–7.68 (m, 2H, H6' and H5'), 8.15 (s, 1H, H5), 8.79 (s, 1H, H2). ^{13}C NMR: δ 57.1 (Ph–O–CH₃), 58.5 (CH₂–O–CH₃), 68.8 (Ph–O–CH₂), 69.9 (CH₃–O–CH₂), 100.5 (C8), 104.4 (C5), 107.2 (C10), 117.0 (d, C3', J C–F = 23.6 Hz), 123.8 (d, C1', J C–F = 12.2 Hz), 125.1 (d, C5', J C–F = 3.08 Hz), 130.1 (C6'), 132.6 (d, C4', J C–F = 9.4 Hz), 135.9 (C4), 149.0 (C2), 150.6 (C9), 159.9 (C7), 158.5 (d, C2', J C–F = 250.5 Hz), 159.2 (C6). MS–ESI *m/z* 378–380 [MH]⁺. Anal. (C₁₈H₁₇N₃O₃ClF·1.0 HCl) C, H, N.

A similar procedure was used to prepare **14**, **21**, **22**, **26**, **72**, and **73**. The heating conditions used were respectively over-

night at 30 °C; 100 °C for 3 h; 110 °C for 4 h; 60 °C for 2 h; 40 °C for 5 h; 50 °C overnight. In the case of **26**, KI (0.28 mmol) was added to facilitate the reaction. In the case of **22**, **72**, and **73**, the crude product was purified by column chromatography prior to hydrochloride salt formation.

***N*-(4-Chloro-2-fluoro-5-hydroxyphenyl)-6-methoxy-7-(2-methoxyethoxy)-4-quinazolinyllamine 13.** 1,1'-Azodicarbonyl-dipiperidine (413 mg, 1.6 mmol) was added portionwise to a stirred mixture of *N*-(5-acetoxy-4-chloro-2-fluorophenyl)-7-hydroxy-6-methoxy-4-quinazolinyllamine **50** (250 mg, 0.66 mmol), 2-methoxyethanol (63 mL, 0.8 mmol), and tributylphosphine (405 mL, 1.6 mmol) in methylene chloride at 0 °C. The resulting solution was allowed to warm to ambient temperature and stirred for 2 h. The solid was removed by filtration, the solvent was removed from the filtrate by evaporation and the residue purified by flash chromatography eluting with acetonitrile/methylene chloride (1:9, increasing in polarity to 4:6) to give 180 mg of *N*-(5-acetoxy-4-chloro-2-fluorophenyl)-7-(2-methoxyethoxy)-6-methoxy-4-quinazolinyllamine (62%) as a solid.

A solution of concentrated aqueous ammonia (5 mL) was added to a solution of *N*-(5-acetoxy-4-chloro-2-fluorophenyl)-7-(2-methoxyethoxy)-6-methoxy-4-quinazolinyllamine (180 mg, 0.4 mmol) in methanol (50 mL). The mixture was stirred at ambient temperature for 3 h and then diluted with water. Most of the methanol was removed by evaporation, and the resulting precipitate collected by filtration, washed with water, and dried to give 73 mg of **13** (45%). Mp >250 °C. ^1H NMR: δ 3.29 (s, 3H, CH₃O), 3.74 (t, 2H, CH₂O), 3.94 (s, 3H, CH₃O), 4.28 (t, 2H, CH₂O), 7.15 (d, 1H, H6'), 7.19 (s, 1H, H5), 7.38 (d, 1H, H3'), 7.77 (s, 1H, H8), 8.36 (s, 1H, H2), 9.40 (s, 1H, OH). MS–ESI *m/z* 394 [MH]⁺. Anal. (C₁₈H₁₇N₃ClFO₄·1.6 H₂O) C, H, N.

***N*-(4-Chloro-2-fluorophenyl)-7-(2-methoxyethoxy)-4-quinazolinyllamine 15. (Procedure C).** A solution of 4-chloro-7-(2-methoxyethoxy)quinazoline hydrochloride **71** (624 mg, 2.27 mmol) and 4-chloro-2-fluoroaniline (305 μL , 2.6 mmol) in 2-propanol (20 mL) was heated at reflux for 30 min. The solvent was removed by evaporation, and the residue partitioned between ethyl acetate and water. The organic layer was separated, washed with aqueous sodium bicarbonate solution, water, dried (MgSO₄), and the solvent removed by evaporation. The residue was triturated with ether to give 662 mg of **15** (84%) as a white solid. Mp 140–141 °C. ^1H NMR: δ 3.35 (s, 3H, CH₃O), 3.74 (t, 2H, CH₂O), 4.29 (t, 2H, CH₂O), 7.21 (s, 1H, H8), 7.28 (d, 1H, H6), 7.35 (d, 1H, H3'), 7.6 (m, 2H, H5' and H6'), 8.36 (d, 1H, H5), 8.43 (s, 1H, H2), 9.75 (s, 1H, NH). ^{13}C NMR: δ 58.1 (CH₂–O–CH₃), 67.4 (Ph–O–CH₂), 70.1 (CH₃–O–CH₂), 107.4 (C8), 109.0 (C10), 116.6 (d, C3', J C–F = 24.2 Hz), 118.1 (C6), 124.5 (d, C5', J C–F = 31 Hz), 124.6 (C5), 125.7 (d, C1', J C–F = 11.5 Hz), 129.3 (C6'), 130.2 (d, C4', J C–F = 10.3 Hz), 152.0 (C9), 155.0 (C2), 156.6 (d, C2', J C–F = 25.1 Hz), 158.0 (C4), 162.0 (C7). MS–ESI *m/z* 347 [MH]⁺. Anal. (C₁₇H₁₅N₃O₂FCl) C, H, N.

***N*-(4-Chloro-2-fluoro-5-hydroxyphenyl)-6-methoxy-7-(2-methoxyethoxy)-4-quinolinylamine hydrochloride 16. (Procedure D).** A suspension of 4-chloro-2-fluoro-5-hydroxyaniline (270 mg, 1.64 mmol) and 4-chloro-6-methoxy-7-(2-methoxyethoxy)quinoline hydrochloride **78** (500 mg, 1.64 mmol) in DMF (6 mL) was heated at 150 °C for 5 h, and the solvent was removed by evaporation. The residue was triturated with ether and collected by filtration. The solid was washed with water, ether and dried under vacuum to give 475 mg of **16** (67%). ^1H NMR: δ 3.37 (s, 3H, CH₃O), 3.8 (t, 2H, CH₂O), 4.03 (s, 3H, CH₃O), 4.31 (t, 2H, CH₂O), 6.5 (m, 1H, H3), 7.2 (d, 1H, H3'), 7.49 (s, 1H, H8), 7.64 (d, 1H, H6'), 8.16 (s, 1H, H5), 8.40 (d, 1H, H2), 10.66 (s, 1H, OH), 10.82 (s, 1H, NH). ^{13}C NMR: δ 56.6 (Ph–O–CH₃), 58.2 (CH₂–O–CH₃), 68.3 (Ph–O–CH₂), 69.8 (CH₂–O–CH₃), 99.9 (C3), 100.4 (C8), 102.7 (C5), 111.5 (C10), 114.9 (C6'), 118.0 (d, C3', J C–F = 23.4 Hz), 118.9 (d, C4', J C–F = 9.4 Hz), 123.8 (d, C1', J C–F = 14.2 Hz), 135.1 (C4), 139.9 (C2), 149.3 (d, C2', J C–F = 237.2 Hz), 149.6 (C6), 150.6 (d, C5', J C–F = 3.5 Hz), 153.1 (C9), 153.9 (C7). MS–ESI *m/z* 393 [MH]⁺. Anal. (C₁₉H₁₈N₂O₄ClF·1.0 HCl) C, H, N.

A similar procedure was used to prepare **17–19**. Reaction mixture were heated respectively for 30, 45, and 20 min.

***N*-(4-Chloro-2-fluorophenyl)-6-methoxy-7-[2-(pyrrolidin-1-yl)ethoxy]-4-quinazolinylamine 20.** 1-(2-chloroethyl)pyrrolidine hydrochloride (200 mg, 1.2 mmol) was added to a mixture of *N*-(4-chloro-2-fluorophenyl)-7-hydroxy-6-methoxy-4-quinazolinylamine **47** (403 mg, 1.26 mmol) and potassium carbonate (650 mg, 4.7 mmol) in DMF (4 mL). The mixture was heated to 100 °C and further portions of 1-(2-chloroethyl)pyrrolidine hydrochloride (800 mg in total) were added periodically over 4 h, while the reaction mixture was maintained at 100 °C. The reaction was then allowed to cool and volatile components were removed by evaporation. The residue was partitioned between methylene chloride and water, separated, and the organic phase passed through phase separating paper. Column chromatography eluting with methylene chloride/methanol (95:5) gave 50 mg of **20** (10%). ¹H NMR: δ 1.8–2.1 (m, 4H, 2-CH₂), 3.1 (m, 2H, CH₂N), 3.55–3.7 (m, 4H, 2-CH₂N), 4.05 (s, 3H, CH₃O), 4.6 (t, 2H, CH₂O), 7.4 (m, 2H, H3' and H8), 7.58 (d, 1H, H5'), 7.65 (dt, 1H, H6'), 8.5 (s, 1H, H5), 8.8 (s, 1H, H2). ¹³C NMR: δ 22.6 (2C, pyrrolidine CH₂), 52.1 (N-CH₂-CH₂-O), 53.9 (2C, pyrrolidine N-CH₂), 57.3 (Ph-O-CH₃), 64.9 (Ph-O-CH₂), 101.0 (C8), 104.68 (C5), 107.6 (C10), 116.9 (d, C3', J_{C-F} = 24.2 Hz), 123.8 (d, C1', J_{C-F} = 12.6 Hz), 125.0 (d, C5', J_{C-F} = 3.2 Hz), 129.8 (C6'), 132.3 (d, C4', J_{C-F} = 10.4 Hz), 135.8 (bs, C4), 149.0 (C2), 150.2 (C9), 154.6 (C7), 156.8 (d, C2', J_{C-F} = 251.9 Hz), 164.8 (C6). MS-ESI *m/z* 417 [MH]⁺. Anal. (C₂₁H₂₂N₄O₂ClF) C, H, N.

***N*-(4-Chloro-2-fluorophenyl)-6-methoxy-7-[4-(4-morpholinyl)butoxy]-4-quinazolinylamine hydrochloride 23.** A solution of *N*-(4-chloro-2-fluorophenyl)-7-(4-chlorobutoxy)-6-methoxy-4-quinazolinylamine **72** (0.1 g, 0.24 mmol) in morpholine (2 mL) was heated at 110 °C for 2 h. After cooling, the mixture was partitioned between ethyl acetate and water. The organic layer was washed with water, brine, dried (MgSO₄), filtered, and evaporated. The resulting oil was purified by column chromatography eluting with methylene chloride/methanol 92:8. The resulting solid was dissolved in methylene chloride and 2 N hydrogen chloride in ether was added (1 mL). The solution was concentrated to a third of its volume and the solid was filtered, washed with ether, and dried under vacuum to give 87 mg of **23** (68%). ¹H NMR (DMSO-*d*₆, CF₃COOD): δ 1.95 (bs, 4H, CH₂CH₂), 3.1 (t, 2H, CH₂O morpholine), 3.25 (bs, 2H, CH₂O morpholine), 3.5 (d, 2H, CH₂O Ar), 3.75 (t, 2H, CH₂N), 3.95 (d, 2H, CH₂N morpholine), 4.03 (s, 3H, CH₃O), 4.28 (t, 2H, CH₂N morpholine), 7.41 (s, 1H, H8), 7.45 (d, 1H, H3'), 7.62 (t, 1H, H6'), 7.68 (dd, 1H, H5'), 8.2 (s, 1H, H5), 8.88 (s, 1H, H2). ¹³C NMR: δ 19.7 (CH₂-CH₂-O), 25.4 (N-CH₂-CH₂), 50.9 (2C, CH₂-N-CH₂), 55.5 (N-CH₂-CH₂), 57.1 (Ph-O-CH₃), 63.1 (2C, CH₂-O-CH₂), 68.6 (Ph-O-CH₂), 100.4 (C8), 104.3 (C5), 107.1 (C10), 116.9 (d, C3', J_{C-F} = 24.0 Hz), 123.8 (d, C1', J_{C-F} = 11.30 Hz), 125.0 (d, C5', J_{C-F} = 4.3 Hz), 129.9 (C6'), 132.3 (d, C4', J_{C-F} = 8.9 Hz), 135.9 (C4), 148.7 (C2), 150.3 (C9), 155.7 (C7), 156.8 (d, C2', J_{C-F} = 253.5 Hz), 158.9 (C6). MS-ESI *m/z* 461 [MH]⁺. Anal. (C₂₃H₂₆ClFN₄O₃·1.3 H₂O, 1.8 HCl) C, H, N.

***N*-(4-Chloro-2-fluorophenyl)-6-methoxy-7-[2-[2-(4-morpholinyl)ethoxy]ethoxy]-4-quinazolinylamine hydrochloride 24. (Procedure E).** Diethyl azodicarboxylate (209 mg, 1.2 mmol) was added dropwise to a mixture of *N*-(4-chloro-2-fluorophenyl)-7-hydroxy-6-methoxy-4-quinazolinylamine **47** (128 mg, 0.4 mmol), triphenylphosphine (314 mg, 1.2 mmol), and 2-(2-morpholinoethoxy)ethanol⁶⁸ (97 mg, 0.56 mmol) in methylene chloride (4 mL) under nitrogen. The mixture was stirred for 1 h at ambient temperature, triphenylphosphine (105 mg, 0.4 mmol), 2-(2-morpholinoethoxy)ethanol (49 mg, 0.28 mmol), and diethyl azodicarboxylate (70 mg, 0.4 mmol) were added. The mixture was stirred for 1 h at ambient temperature and was purified by pouring directly onto a silica column eluting with methylene chloride/acetonitrile/methanol (6:3:1). The purified product was triturated with ether, collected by filtration, and dissolved in methylene chloride. 2 N hydrogen chloride in ether (0.5 mL) was added, and the resulting precipitate was collected by filtration, washed with

ether, and dried under vacuum to give 100 mg of **24** (45%). ¹H NMR (DMSO-*d*₆, CF₃COOD): δ 3.1–3.2 (m, 2H, CH₂N), 3.3–3.5 (m, 5H, 2-CH₂N and CHO), 3.7–3.8 (m, 2H, CH₂O), 3.9–4.0 (m, 5H, CH₂O), 4.02 (s, 3H, CH₃O), 4.4 (br s, 2H, CH₂O), 7.46 (s, 1H, H8), 7.48 (d, 1H, H3'), 7.6 (t, 1H, H6'), 7.7 (d, 1H, H5'), 8.25 (s, 1H, H5), 8.89 (s, 1H, H2). MS-ESI *m/z* 477 [MH]⁺. Anal. (C₂₃H₂₆N₄O₄ClF·1.0 H₂O, 1.95 HCl) C, H, N.

A similar procedure was used to synthesize **25** and **35**.

***N*-(4-Chloro-2-fluorophenyl)-7-[2-(1-imidazolyl)ethoxy]-6-methoxy-4-quinazolinylamine hydrochloride 27. (Procedure F).** A solution of 1,1'-(azodicarbonyl)dipiperidine (378 mg, 1.5 mmol) in methylene chloride (5 mL) was added dropwise to a suspension of *N*-(4-chloro-2-fluorophenyl)-7-hydroxy-6-methoxy-4-quinazolinylamine **47** (160 mg, 0.5 mmol), tributylphosphine (303 mg, 1.5 mmol), and 2-(imidazol-1-yl)ethanol (67 mg, 0.6 mmol)⁶⁹ in methylene chloride (8 mL), and the mixture was stirred for 3 h at ambient temperature. Acetic acid (60 mg, 1 mmol) was added, and the solvent was removed by evaporation. The solid residue was adsorbed on silica and purified by column chromatography eluting with methylene chloride/methanol (9:1 followed by 8:2). The resulting white solid was dissolved in methylene chloride/methanol and a solution of 5 N hydrogen chloride in 2-propanol was added. The solvent was removed by evaporation and the solid was triturated with ether, filtered, washed with ether, and dried under vacuum to give **27** (180 mg, 74%). mp 218–221 °C. ¹H NMR: δ 4.01 (s, 3H, CH₃O), 4.62 (t, 2H, CH₂O), 4.76 (t, 2H, CH₂N), 7.44 (dd, 1H, H3'), 7.48 (s, 1H, H8), 7.59 (t, 1H, H6'), 7.66 (dd, 1H, H5'), 7.72 (s, 1H, imidazole H4), 7.84 (s, 1H, imidazole H5), 8.41 (s, 1H, H5), 8.78 (s, 1H, H2), 9.22 (s, 1H, imidazole H2). MS-ESI *m/z* 414 [MH]⁺. Anal. (C₂₀H₁₇N₅O₂ClF·0.4 H₂O, 2.0 HCl) C, H, N.

***N*-(4-Chloro-2-fluorophenyl)-6-methoxy-7-[2-[1-(1,2,4-triazolyl)ethoxy]-4-quinazolinylamine hydrochloride 29. (Procedure G).** Diethylazodicarboxylate (295 μL, 1.8 mmol) was added dropwise to a solution of *N*-(4-chloro-2-fluorophenyl)-7-hydroxy-6-methoxy-4-quinazolinylamine **47** (300 mg, 0.93 mmol), 2-(1,2,4-triazol-1-yl)ethanol⁷⁰ (159 mg, 1.4 mmol), and triphenylphosphine (492 mg, 1.8 mmol) in methylene chloride (10 mL). The mixture was stirred for 2 h at ambient temperature and further triphenylphosphine (246 mg, 0.9 mmol) and diethylazodicarboxylate (147 μL, 0.9 mmol) were added. The mixture was stirred for 1 h at ambient temperature, and the resulting precipitate was collected by filtration, washed with methylene chloride and ether, and dried under vacuum. This solid was suspended in methylene chloride/methanol and a 5 M solution of hydrogen chloride in 2-propanol (1.0 mL) was added. The volatiles were removed by evaporation, and the residue was triturated with ether. The resulting solid was collected by filtration, washed with ether, and dried under vacuum to give 219 mg of **29** (52%). Mp 169–174 °C. ¹H NMR: δ 3.99 (s, 3H, CH₃O), 4.60 (t, 2H, CH₂N), 4.74 (t, 2H, CH₂O), 7.43 (d, 1H, H3'), 7.45 (s, 1H, H8), 7.59 (t, 1H, H6'), 7.67 (dd, 1H, H5'), 8.06 (s, 1H, triazole), 8.41 (s, 1H, H5), 8.68 (s, 1H, triazole), 8.83 (s, 1H, H2). MS-ESI *m/z* 415 [MH]⁺. Anal. (C₁₉H₁₆N₆O₂ClF·1.6 H₂O, 1.0 HCl, 0.35 tPrOH) C, H, N.

***N*-(4-Bromo-2-fluorophenyl)-6-methoxy-7-[2-(1*H*,1,2,3-triazol-1-yl)ethoxy]-4-quinazolinylamine hydrochloride 34.** To a solution of *N*-(4-bromo-2-fluorophenyl)-7-hydroxy-6-methoxy-4-quinazolinylamine **49** (0.13 g, 0.357 mmol) in methylene chloride (4 mL) was added triphenylphosphine (0.28 g, 1.07 mmol) and 2-hydroxyethyl-1-(1,2,3-triazole)⁷¹ (60 mg, 0.53 mmol) followed by diethylazodicarboxylate (0.17 mg, 1.08 mmol) dropwise. After the solution was stirred for 1 h at ambient temperature, triphenylphosphine (95 mg, 0.36 mmol), 2-hydroxyethyl-1-(1,2,3-triazole) (20 mg, 0.177 mmol) and diethylazodicarboxylate (60 μL, 0.381 mmol) was added. After the solution was stirred for 1 h at ambient temperature, the precipitate formed was filtered. The solid was suspended in a mixture of methylene chloride/methanol 1:1 and 3.8 N hydrogen chloride in ether (0.5 mL) was added. The solution was diluted with ether. The precipitate was filtered, washed with ether, and dried under vacuum at 70 °C to give 96 mg of **34**

(54%). ¹H NMR spectrum (DMSO-*d*₆, CF₃COOD): δ 3.98 (s, 3H, CH₃O), 4.69 (t, 2H, CH₂O), 4.95 (t, 2H, CH₂N), 7.35 (s, 1H, H8), 7.5–7.65 (m, 2H, H6' or H3'), 7.78 (s, 1H, triazole), 7.82 (d, 1H, H5'), 8.07 (s, 1H, triazole), 8.21 (s, 1H, H5), 8.87 (s, 1H, H2). ¹³C NMR: δ 48.7 (N–CH₂), 56.4 (Ph–O–CH₃), 67.1 (Ph–O–CH₂), 102.5 (C5), 108.4 (C8), 109.2 (C10), 117.8 (d, C4', *J*C–F = 9.1 Hz), 119.5 (d, C3', *J*C–F = 23.4 Hz), 125.5 (triazole C5), 126.5 (d, C1', *J*C–F = 12.3 Hz), 127.7 (d, C6', *J*C–F = 2.9 Hz), 129.7 (d, C5', *J*C–F = 2.1 Hz), 133.6 (triazole C4), 146.9 (C9), 149.1 (C6), 153.0 (C7), 153.2 (C2), 156.8 (d, C2', *J*C–F = 251.5 Hz), 157.1 (C4). MS–ESI *m/z* 459–461 [MH]⁺. Anal. (C₁₉H₁₆BrFN₆O₂·0.46 H₂O, 0.85 HCl) C, H, N.

N-[4-(4-Chloro-2-fluoroanilino)-6-methoxy-7-quinazoliny]-2-methoxyacetamide hydrochloride 31. To a suspension of *N*-(2-fluoro-4-chlorophenyl)-7-amino-6-methoxy-4-quinazolinyamine **66** (0.4 g, 1.1 mmol) and pyridine (5 mL) in methylene chloride (8 mL) cooled at 5 °C was added methoxyacetyl chloride (123 μL, 1.3 mmol). After the solution was stirred for 2 h at ambient temperature, the volatile components were removed by evaporation. The residue was triturated with water and filtered. The solid was azeotroped successively with ethanol and toluene. The crude product was purified by column chromatography, eluting with methylene chloride/acetonitrile/methanol 60:38:2. After evaporation of the solvent, the solid was dissolved in methylene chloride and 3 N hydrogen chloride in 2-propanol was added. The volatiles were removed by evaporation, and the solid was filtered and washed with 2-propanol, followed by ether and dried under vacuum to give 119 mg of **31** (40%). ¹H NMR: δ 3.45 (s, 2H, CH₂), 4.12 (s, 3H, CH₃O), 4.19 (s, 3H, CH₃O), 7.45 (d, 1H, H3'), 7.6 (t, 1H, H6'), 7.7 (d, 1H, H5'), 8.4 (s, 1H, H8), 8.8 (s, 1H, H5), 8.9 (s, 1H, H2), 9.52 (s, 1H, NH), 11.52 (bs, 1H, NH). ¹³C NMR: δ 57.8 (Ph–O–CH₃), 85.8 (CH₂–O–CH₃), 71.4 (C=OCH₂–O), 104.2 (C8), 106.9 (C5), 108.8 (C10), 116.9 (d, C3, *J*C–F = 23.6 Hz), 123.7 (d, C1', *J*C–F = 12.4 Hz), 126.0 (d, C5', *J*C–F = 4.2 Hz), 129.8 (C6), 132.4 (d, C4', *J*C–F = 9.7 Hz), 134.9 (C4), 135.2 (C7), 148.7 (C2), 149.3 (C9), 156.8 (d, C2', *J*C–F = 252.1 Hz), 159.2 (C6), 169.2 (C=O). MS–ESI *m/z* 391 [MH]⁺. Anal. (C₁₈H₁₆ClFN₄O₃·0.7 HCl 1.5 H₂O) C, H, N.

A similar procedure was used to synthesize **28** and **30**.

N-(4-Chloro-2-fluorophenyl)-6-methoxy-7-[(1-methyl-4-piperidinyl)oxy]-4-quinazolinyamine 32. (Procedure H). To a suspension of *N*-(4-chloro-2-fluorophenyl)-7-hydroxy-6-methoxy-4-quinazolinyamine **47** (159 mg, 0.5 mmol) in methylene chloride (5 mL) cooled at 5 °C was added triphenylphosphine (328 mg, 1.25 mmol), and *N*-methyl-4-hydroxypiperidine (115 mg, 1 mmol), followed by diethylazodicarboxylate (218 mg, 1.25 mmol) dropwise. After the solution stirred for 1 h at ambient temperature, the volatiles were removed by evaporation and the residues were partitioned between ether and 2 N aqueous hydrochloric acid. The aqueous layer was washed with ether and the pH was adjusted to 9 with aqueous sodium bicarbonate. The aqueous layer was extracted with methylene chloride. The organic layer was washed with brine, dried (MgSO₄), and evaporated. The residue was purified by column chromatography on neutral alumina eluting with methylene chloride/methanol 97:3. After evaporation of the solvent, the solid was dissolved in methylene chloride and 3 N hydrogen chloride in 2-propanol was added. The volatiles were removed by evaporation and the solid was filtered, washed with 2-propanol, followed by ether and dried under vacuum to give 180 mg of **32** (79%). ¹H NMR (DMSO-*d*₆, CD₃COOD): δ 1.9–2.0 (m, 1H), 2.15–2.25 (m, 2H), 2.35–2.45 (m, 1H), 2.82 and 2.85 (2s, 3H, CH₃N), 3.05–3.25 (m, 2H), 3.4–3.5 (d, 1H), 3.55–3.65 (d, 1H), 4.0 and 4.05 (2s, 3H, CH₃O), 4.85 (m, 0.5H), 5.0 (bs, 0.5H), 7.45 (d, 1H, H3'), 7.5 (s, 0.5H, H8), 7.58 (s, 0.5H, H8), 7.6 (t, 1H, H6'), 7.68 (dd, 1H, H5'), 8.18 (s, 0.5H, H5), 8.2 (s, 0.5H, H5), 8.9 (s, 1H, H2). MS–ESI *m/z* 417 [MH]⁺. Anal. (C₂₁H₂₂N₄O₂Cl₃·1.8 HCl, 0.4 H₂O) C, H, N.

N-(2-Fluoro-5-hydroxy-4-methylphenyl)-6-methoxy-7-methoxyacetamido-4-quinazolinyamine hydrochloride 33. 2 N aqueous sodium hydroxide solution (620 μL) was added

dropwise to a suspension of *N*-(2-fluoro-5-methoxycarbonyloxy-4-methylphenyl)-6-methoxy-7-methoxyacetamido-4-quinazolinyamine **68** (275 mg, 0.62 mmol) in methanol (8 mL) at 5 °C, and the mixture then stirred for 90 min at ambient temperature. The reaction mixture was diluted with water and adjusted to pH 7 with 2 N hydrogen chloride. The precipitated solid was collected by filtration, resuspended in ethanol and a 5 N solution of hydrogen chloride in 2-propanol (0.3 mL) added. The volatiles were removed from the resulting solution by evaporation, and the solid washed with ether collected by filtration and dried under vacuum to give 216 mg of **33** (82%). Mp 300–306 °C. ¹H NMR: δ 2.18 (s, 3H, CH₃–Ar), 3.47 (s, 3H, CH₃O), 4.13 (s, 3H, CH₃O), 4.21 (s, 2H, CH₂O), 6.92 (d, 1H, H6' or H3'), 7.13 (d, 1H, H3' or H6'), 8.41 (s, 1H, H8), 8.80 (s, 1H, H5), 8.90 (s, 1H, H2), 9.54 (s, 1H, NH or OH), 9.72 (s, 1H, NH or OH), 11.49 (s, 1H, NH). ¹³C NMR: δ 15.7 (Ph–O–CH₃), 57.6 (CO–CH₂–O), 71.4 (C=OCH₂–O), 104.0 (C8), 106.8 (C5), 108.6 (C10), 113.4 (C6'), 117.3 (d, C3', *J*C–F = 20.6 Hz), 121.2 (d, C1', *J*C–F = 14.2 Hz), 125.1 (d, C4', *J*C–F = 7.7 Hz), 134.6 (C4), 135.0 (C7), 148.6 (C2), 149.3 (C9), 149.7 (d, C2', *J*C–F = 238.4 Hz), 151.5 (d, C5', *J*C–F = 1.7 Hz), 159.2 (C6), 169.2 (C=O). MS–ESI *m/z* 387 [MH]⁺. Anal. (C₁₉H₁₉N₄O₄F·1.0 HCl, 0.6 H₂O) C, H, N.

N-(4-Cyano-2-fluorophenyl)-6-methoxy-7-[2-(1H-1,2,3-triazol-1-yl)ethoxy]-4-quinazolinyamine hydrochloride 36. A solution of 4-chloro-6-methoxy-7-[2-(1,2,3-triazol-1-yl)ethoxy]quinazoline **58** (170 mg, 0.56 mmol) and 4-cyano-2-fluoroaniline⁷² (91 mg, 0.67 mmol) in 2-propanol (8 mL) containing 3 N hydrogen chloride in 2-propanol (0.2 mL) was refluxed for 2.5 h. After the solution was cooled to ambient temperature, methylene chloride (20 mL) and methanol (20 mL) were added. A21 amberlyste resin was added until pH = 8. The mixture was filtered. Silica was added to the filtrate and the solvents were removed under vacuum. The residue was poured onto a silica column and eluted successively with methylene chloride; methylene chloride/ethyl acetate 1:1 and methylene chloride/ethyl acetate/methanol 6:4:1. After removal of the solvent, the residue was dissolved in methylene chloride/methanol (5:1) and 3 N hydrogen chloride in ether (0.5 mL) was added. The volatiles were removed by evaporation and the residue was filtered, washed with ether, and dried under vacuum to give 72 mg of **36** (28%). ¹H NMR (DMSO-*d*₆, CF₃COOD): 4.01 (s, 3H, CH₃O), 4.71 (t, 2H, CH₂O), 4.98 (t, 2H, CH₂N), 7.40 (s, 1H, H5), 7.8 (s, 1H, triazole), 7.8–7.9 (m, 2H, H3' and H6'), 8.1 (d, 1H, H5'), 8.15 (s, 1H, triazole), 8.25 (s, 1H, H8), 8.93 (s, 1H, H2). ¹³C NMR: δ 48.5 (CH₂–N), 57.3 (Ph–O–CH₃), 67.8 (Ph–O–CH₂), 101.1 (C8), 104.7 (C5), 107.9 (C10), 110.8 (d, C4', *J*C–F = 10.8 Hz), 117.7 (d, CN, *J*C–F = 2.3 Hz), 120.6 (d, C3', *J*C–F = 23.4 Hz), 125.6 (triazole C5), 129.5 (d, C5' or C6', *J*C–F = 3.5 Hz), 129.6 (C6' or 5'), 130.1 (d, C1', *J*C–F = 11.4 Hz), 136.3 (C4), 149.1 (C2), 150.6 (C9), 155.3 (C7), 156.3 (d, C2', *J*C–F = 252.2 Hz), 158.9 (C6). MS–ESI *m/z* 406 [MH]⁺. Anal. (C₂₀H₁₆FN₇O₂·1.25 HCl, 0.3 H₂O) C, H, N.

4-Chloro-6,7-dimethoxyquinazoline hydrochloride 38²⁵. (Procedure I). A solution of 6,7-dimethoxy-3,4-dihydroquinazolin-4-one **37** (2.06 g, 10 mmol) in thionyl chloride (20 mL) containing DMF (2 drops) was stirred and heated to reflux for 2 h. The mixture was evaporated and the residue was triturated with ether, filtered, and dried under vacuum to give 2 g of **38** (90%). ¹H NMR: δ 4.0 (s, 3H, CH₃O), 4.01 (s, 3H, CH₃O), 7.40 (s, 1H, H8 or H5), 7.46 (s, 1H, H8 or H5), 8.88 (s, 1H, H2). MS–EI *m/z* 224–226 [M]⁺.

A similar procedure was used to prepare **40**, **56**, **58**, **63**, **71**, and **78**. In the case of **56** and **58**, the free base of the chloroquinazoline was generated by treatment with sodium bicarbonate.

7-Benzyloxy-6-methoxy-3,4-dihydroquinazolin-4-one 40. A mixture of 2-amino-4-benzyloxy-5-methoxybenzamide **39**²⁶ (10 g, 40 mmol) and Gold's reagent (7.4 g, 50 mmol) in dioxane (100 mL) was stirred and heated at reflux for 24 h. Sodium acetate (3.02 g, 37 mmol) and acetic acid (1.65 mL, 29 mmol) were added to the reaction mixture and it was heated for a further 3 h. The volatile components were removed by evapo-

ration, water was added to the residue, the solid was collected by filtration, washed with water, and dried. Recrystallization from acetic acid gave 8.7 g of **40** (84%). Mp 266 °C. ¹H NMR: δ 3.85 (s, 3H, CH₃O), 5.25 (s, 2H, CH₂O), 7.25 (s, 1H, H8), 7.4 (m, 6H, Ph and H5), 7.95 (s, 1H, H2), 12.0 (br s, 1H, NH). ¹³C NMR: δ 55.7 (CH₂O), 70.0 (OCH₃), 105.1 (C5), 109.3 (C8), 115.7 (C10), 127.9 (2 C12), 128.0 (C14), 128.5 (2 C13), 136.3 (C11), 143.8 (C2), 144.7 (C6), 148.7 (C7), 153.3 (C9), 160.0 (C4). MS-ESI *m/z* 305 [MNa]⁺. Anal. (C₁₆H₁₄N₂O₃·0.24 H₂O) C, H, N.

N-7-Benzoyloxy-(4-chloro-2-fluorophenyl)-6-methoxy-4-quinazolinylamine hydrochloride 42. (Procedure J). A solution of 7-Benzoyloxy-4-chloro-6-methoxyquinazoline hydrochloride **41** (1.2 g, 3.5 mmol) and 4-chloro-2-fluoroaniline (444 μL, 4 mmol) in 2-propanol (40 mL) was refluxed for 1.5 h. After the solution was cooled, the precipitate was collected by filtration, washed with 2-propanol then ether and dried under vacuum to give 1.13 g of **42** (71%). Mp 239–242 °C. ¹H NMR: δ 4.0 (s, 3H, CH₃O), 5.36 (s, 2H, CH₂O), 7.39–7.52 (m, 9H, Ph and H3', H5', H6' and H8), 8.1 (s, 1H, H5), 8.75 (s, 1H, H2). ¹³C NMR: δ 57.0 (O-CH₃), 70.7 (O-CH₂), 100.8 (C8), 104.3 (C5), 107.1 (C10), 116.9 (d, C3', *J*C-F = 23.8 Hz), 123.8 (d, C1', *J*C-F = 13.4 Hz), 125.0 (d, C5', *J*C-F = 3.0 Hz), 128.3 (C13), 128.4 (C14), 128.6 (C12), 129.9 (C6'), 132.4 (d, C4', *J*C-F = 9.1 Hz), 135.2 (C11), 135.5 (C4), 148.8 (C2), 150.5 (C9), 155.4 (C7), 156.8 (d, C2', *J*C-F = 252.2 Hz), 159.0 (C6). MS-ESI *m/z* 410 [MH]⁺. Anal. (C₂₂H₁₇N₃O₂ClF·1.0 HCl) C, H, N.

A similar procedure was used to prepare **43–45**. In the case of **44** and **45**, the mixture was heated for 4 h and 2 h, respectively.

N-(5-Acetoxy-4-chloro-2-fluorophenyl)-7-benzoyloxy-6-methoxy-4-quinazolinylamine 46. Triethylamine (216 mL, 1.5 mmol) and acetic anhydride (133 mL, 1.4 mmol) were added to a stirred suspension of *N*-7-benzoyloxy-(4-chloro-2-fluoro-5-hydroxyphenyl)-6-methoxy-4-quinazolinylamine hydrochloride **45** (600 mg, 1.4 mmol) in methylene chloride (7 mL). The mixture was stirred at ambient temperature for 3 h and insoluble material removed by filtration. Volatiles were removed from the filtrate by evaporation, and the residue purified by flash chromatography, eluting with methylene chloride/methanol (100:0, increasing in polarity to 97:3) to give 340 mg of **46** (52%). ¹H NMR: δ 2.34 (s, 3H, CH₃CO), 3.94 (s, 3H, CH₃O), 5.28 (s, 2H, CH₂O), 7.28 (s, 1H, H8), 7.35–7.44 (m, 2H, H3' and H14), 7.50 (d, 2H, H12), 7.58 (d, 1H, H6'), 7.70 (d, 1H, H13), 7.80 (s, 1H, H5), 8.37 (s, 1H, H5'), 9.30 (s, 1H, H2). MS-ESI *m/z* 468 [MH]⁺.

N-(4-Chloro-2-fluorophenyl)-7-hydroxy-6-methoxy-4-quinazolinylamine 47. (Procedure K). A solution of *N*-(4-chloro-2-fluorophenyl)-7-benzoyloxy-6-methoxy-4-quinazolinylamine hydrochloride **42** (892 mg, 2 mmol) in TFA (10 mL) was refluxed for 50 min. After the solution was cooled, the mixture was poured onto ice. The precipitate was collected by filtration, dissolved in methanol (10 mL) and basified to pH = 11 with aqueous ammonia. After concentration by evaporation, the solid product was collected by filtration, washed with water then ether and dried under vacuum to give 460 mg of **47** (72%). Mp 141–143 °C. ¹H NMR: δ 3.95 (s, 3H, CH₃O), 7.05 (s, 1H, H8), 7.35 (d, 1H, H3'), 7.54–7.59 (m, 2H, H5' and H6'), 7.78 (s, 1H, H5), 8.29 (s, 1H, H2). ¹³C NMR: δ 56.1 (CH₂O), 101.2 (C5), 108.6 (C8), 108.8 (C10), 111.9 (d, C3', *J*C-F = 23.9 Hz), 116.6 (d, C1', *J*C-F = 18.4 Hz), 119.9 (d, C5', *J*C-F = 3.7 Hz), 130.9 (C6'), 147.6 (C7), 150.2 (C6), 151.5 (C2), 151.9 (d, C4', *J*C-F = 11.0 Hz), 155.2 (C9), 157.3 (d, C2', *J*C-F = 246.3 Hz), 164.6 (C4). MS-ESI *m/z* 320–322 [MH]⁺.

A similar procedure was used to prepare **48** and **49**.

N-(5-Acetoxy-4-chloro-2-fluorophenyl)-7-hydroxy-6-methoxy-4-quinazolinylamine 50. A solution of *N*-(5-acetoxy-4-chloro-2-fluorophenyl)-7-benzoyloxy-6-methoxy-4-quinazolinylamine **46** (250 mg, 0.54 mmol) in methanol (5 mL), chloroform (5 mL), and DMF (1 mL) was stirred under hydrogen at 1 atm with 5% palladium-on-charcoal catalyst (100 mg) for 4 h. The catalyst was removed by filtration through diatomaceous earth and the solvent removed by evaporation. The residue was dissolved in ethyl acetate,

washed with water and brine, and dried (MgSO₄). Most of the solvent was removed by evaporation, the mixture was cooled, and hexane added to obtain a solid product that was collected by filtration, washed with hexane/ethyl acetate, and dried to give 170 mg of **50** (45%). ¹H NMR: δ 2.37 (s, 3H, CH₃CO), 3.95 (s, 3H, CH₃O), 7.08 (s, 1H, H3'), 7.59 (s, 1H, H8), 7.68 (d, 1H, H6'), 7.78 (s, 1H, H5), 8.34 (s, 1H, H2), 9.48 (s, 1H, NH or OH). ¹³C NMR δ 15.1 (Ar CH₃), 55.6 (COOCH₃), 56.0 (OCH₃), 102.2 (C5), 108.0 (C10), 110.0 (C8), 117.5 (d, C3', *J*C-F = 22.0 Hz), 121.1 (d, C6', *J*C-F = 2.3 Hz), 125.0 (d, C3', *J*C-F = 14.7 Hz), 128.4 (d, C6', *J*C-F = 7.4 Hz), 144.6 (C6 or C7), 144.7 (C7 or C6), 148.6 (C9), 152.8 (C2), 153.3 (O-C=O), 154.3 (d, C2', *J*C-F = 244.6 Hz), 157.0 (C4). MS-ESI *m/z* 394 [MH]⁺.

7-Benzoyloxy-6-methoxy-3-(pivaloyloxymethyl)-3,4-dihydroquinazolin-4-one 51. Sodium hydride (1.44 g of a 60% suspension in mineral oil, 36 mmol) was added in portions over 20 min to a solution of 7-benzoyloxy-6-methoxy-3,4-dihydroquinazolin-4-one **40** (8.46 g, 30 mmol) in DMF (70 mL) and the mixture was stirred for 1.5 h. Chloromethyl pivalate (5.65 g, 37.5 mmol) was added dropwise and the mixture stirred for 2 h at ambient temperature. The mixture was diluted with ethyl acetate (100 mL) and poured onto ice-water (400 mL) and 2 N hydrochloric acid (4 mL). The organic layer was separated and the aqueous layer extracted with ethyl acetate, the combined extracts were washed with brine, dried (MgSO₄), and the solvent removed by evaporation. The residue was triturated with a mixture of ether and petroleum ether, the solid was collected by filtration, and dried under vacuum to give 10 g of **51** (84%). ¹H NMR: δ 1.11 (s, 9H, C(CH₃)₃), 3.89 (s, 3H, CH₃O), 5.3 (s, 2H, OCH₂N), 5.9 (s, 2H, CH₂Oph), 7.27 (s, 1H, H8), 7.35 (m, 1H, H14), 7.47 (t, 2H, H13), 7.49 (d, 2H, H12), 7.51 (s, 1H, H5), 8.34 (s, 1H, H2). ¹³C NMR: δ 26.5 (C-(CH₃)₃), 38.3 (C-Me₃), 55.8 (OCH₃), 69.0 (NCH₂O), 70.1 (OCH₃), 105.6 (C5), 109.5 (C8), 114.4 (C10), 127.9 (2 C13), 128.1 (C14), 128.5 (2 C12), 136.1 (C11), 143.6 (C6), 146.3 (C2), 149.1 (C7), 153.8 (C9), 159.0 (C4), 177.0 (O-C=O). MS-ESI *m/z* 397 [MH]⁺. Anal. (C₂₂H₂₄N₂O₅·0.5 H₂O) C, H, N.

7-Hydroxy-6-methoxy-3-(pivaloyloxymethyl)-3,4-dihydroquinazolin-4-one 52. A mixture of 7-benzoyloxy-6-methoxy-3-(pivaloyloxymethyl)-3,4-dihydroquinazolin-4-one **51** (7 g, 17.7 mmol) and 10% palladium-on-charcoal catalyst (700 mg) in ethyl acetate (250 mL), DMF (50 mL), methanol (50 mL), and acetic acid (0.7 mL) was stirred under hydrogen at atmospheric pressure for 40 min. The catalyst was removed by filtration and the solvent removed from the filtrate by evaporation. The residue was triturated with ether, collected by filtration, and dried under vacuum to give 4.36 g of **52** (80%). ¹H NMR: δ 1.1 (s, 9H, C(CH₃)₃), 3.89 (s, 3H, CH₃O), 5.89 (s, 2H, OCH₂N), 7.0 (s, 1H, H8), 7.48 (s, 1H, H5), 8.5 (s, 1H, H2). ¹³C NMR: δ 26.5 (C-(CH₃)₃), 38.3 (C-Me₃), 55.8 (OCH₃), 69.0 (NCH₂O), 106.0 (C5), 111.4 (C8), 113.3 (C10), 143.8 (C7 or C6), 146.1 (C2), 148.5 (C6 or C7), 153.6 (C9), 159.0 (C4), 177.0 (O-C=O). MS-ESI *m/z* 329 [MNa]⁺. Anal. (C₁₅H₁₈N₂O₅·0.3 H₂O, 0.02 DMF) C, H, N.

7-(2-Methoxyethoxy)-6-methoxy-3-(pivaloyloxymethyl)-3,4-dihydroquinazolin-4-one 53. (Procedure L). Diethylazodicarboxylate (1.16 mL, 7.35 mmol) was added dropwise to a solution of 7-hydroxy-6-methoxy-3-(pivaloyloxymethyl)-3,4-dihydroquinazolin-4-one **52** (1.5 g, 4.9 mmol) in dichloromethane (15 mL) containing triphenylphosphine (1.93 g, 7.35 mmol) and 2-methoxyethanol (0.46 mL, 5.88 mmol). After the solution was stirred for 1 h at ambient temperature, the volatiles were removed under vacuum. The solid was purified by column chromatography eluting with ethyl acetate/petroleum ether (1:1) followed by 3:2. After evaporation of the solvent, the solid was triturated with ether, filtered and dried under vacuum to give 1.5 g of **53** (84%). ¹H NMR: δ 1.13 (s, 9H, tBu), 3.35 (s, 3H, CH₃O), 3.72 (m, 2H, CH₂O), 3.9 (s, 3H, CH₃O), 4.3 (m, 2H, CH₂O), 5.92 (s, 2H, NCH₂O), 7.2 (s, 1H, H8), 7.51 (s, 1H, H5), 8.37 (s, 1H, H2). ¹³C NMR: δ 26.5 (C(CH₃)₃), 38.1 (C(CH₃)₃), 55.7 (PhOCH₃), 58.2 (CH₂-O-CH₃), 68.0 (N-CH₂-O), 69.0 (Ph-CH₂-O), 70.0 (CH₂-O-CH₃), 105.4 (C5 or C8), 108.9 (C8 or C5), 114.3 (C10), 143.6 (C6 or

C7), 146.3 (C2), 148.9 (C7 or C6), 154.1 (C9), 159.0 (C4), 177.0 (O—C=O). MS—ESI m/z 365 [MH]⁺. Anal. (C₁₈H₂₄O₆N₂·0.18 H₂O) C, H, N.

A similar procedure was used to prepare **54**.

6-Methoxy-[7-(2-methoxyethoxy)]-3,4-dihydroquinazolin-4-one 55. (Procedure M). A suspension of 6-methoxy-[7-(2-methoxyethoxy)]-3-[(pivaloyloxy)methyl]-3,4-dihydroquinazolin-4-one **53** (1.35 g, 3.7 mmol) in 7 N ammonia in methanol (50 mL) was stirred at ambient temperature overnight. After removal of the volatiles under vacuum, the residue was triturated with ether, filtered, washed with ether followed by ether/methylene chloride/methanol 7:3:1 and dried under vacuum to give 810 mg of **55** (87%). ¹H NMR: δ 3.35 (s, 3H, CH₃O), 3.75 (m, 2H, CH₂O), 3.9 (s, 3H, CH₃O), 4.24 (m, 2H, CH₂O), 7.15 (s, 1H, H8), 7.46 (s, 1H, H5), 7.99 (s, 1H, H2). ¹³C NMR: δ 55.6 (Ph—O—CH₃), 58.2 (CH₂—O—CH₃), 67.9 (Ph—O—CH₂), 70.0 (CH₂—O—CH₃), 105.0 (C5), 108.7 (C8), 115.6 (C10), 143.8 (C2), 147.7 (C6), 148.5 (C7), 153.6 (C9), 160.0 (C4). MS—ESI m/z 251 [MH]⁺. Anal. (C₁₂H₁₄O₄N₂·0.1 H₂O) C, H, N.

A similar procedure was used to prepare **57**.

N-(4-Chloro-2-fluorophenyl)-6,7-dihydroxy-4-quinazolinylamine 59. A mixture of *N*-(4-chloro-2-fluorophenyl)-7-hydroxy-6-methoxy-4-quinazolinylamine **47** (0.5 g, 1.5 mmol) and pyridine hydrochloride (3.6 g, 31 mmol) was melted at 190–220 °C for 1 h. After the solution was cooled, the solid was suspended in water (60 mL) and sonicated for 15 min. The solid was filtered, washed with water followed by ether, and dried under vacuum to give 383 mg of **59** (84%). ¹H NMR: δ 7.42 (s, 2H, H8 and H3'), 7.55 (t, 1H, H6'), 7.65 (d, 1H, H5'), 7.93 (s, 1H, H5), 8.69 (s, 1H, H2), 10.2–10.7 (br s, 1H, NH), 11.0 (bs, 2H, OH). MS—ESI m/z 306 [MH]⁺. Anal. (C₁₄H₉N₃O₂·FCI·0.75 HCl) C, H, N.

2-Amino-5-methoxy-4-nitrobenzoic acid 61. A solution of 2-acetamido-5-methoxy-4-nitrobenzoic acid **60** (21.6 g, 85 mmol) in water (76 mL) and concentrated hydrochloric acid (30.5 mL) was heated at reflux for 3 h. The reaction mixture was cooled to 0 °C, the resulting solid was collected by filtration, washed with water and dried under vacuum to give 16.6 g of **61** (92%). ¹H NMR δ 3.79 (s, 3H, CH₃O), 7.23 (s, 1H, H6), 7.52 (s, 1H, H3), 8.8 (br s, 2H, NH₂).

6-Methoxy-7-nitro-3,4-dihydroquinazolin-4-one 62. A solution of 2-amino-5-methoxy-4-nitrobenzoic acid **61** (16.6 g, 78 mmol) in formamide (250 mL) was heated at reflux for 4.5 h. The reaction mixture was cooled to 0 °C, diluted with water, and the resulting precipitate collected by filtration, washed with water, and dried under vacuum to give 11.56 g of **62** (67%). ¹H NMR (DMSO-*d*₆, CF₃COOD): δ 4.02 (s, 3H, CH₃O), 7.8 (s, 1H, H8), 8.12 (s, 1H, H2 or H5), 8.18 (s, 1H, H2 or H5). MS—ESI m/z 222 [MH]⁺. Anal. (C₉H₇N₃O₄·0.3 H₂O) H, N, C: calcd 47.71, found 47.3.

N-7-Amino-(4-chloro-2-fluorophenyl)-6-methoxy-4-quinazolinylamine 66. A solution of *N*-(4-chloro-2-fluorophenyl)-6-methoxy-7-nitro-4-quinazolinylamine hydrochloride **64** (6 g, 15 mmol) in a mixture of DMF (100 mL) and methanol (600 mL) containing 10% Pd/C (1.8 g) was hydrogenated at 1.3 atm for 2 h. After filtration, the filtrate was evaporated. The solid residue was triturated with a mixture of methylene chloride and ether, filtered, washed with ether, and dried under vacuum to give **66**, which was used without purification in the next stage. MS—ESI m/z 319 [MH]⁺.

N-7-Amino-(2-fluoro-5-methoxycarbonyloxy-4-methylphenyl)-6-methoxy-4-quinazolinylamine hydrochloride 67. A mixture of *N*-(2-fluoro-5-methoxycarbonyloxy-4-methylphenyl)-6-methoxy-7-nitro-4-quinazolinylamine hydrochloride **65** (1.1 g, 25 mmol) and 10% palladium-on-charcoal catalyst (220 mg) in methanol (200 mL) and ethanol (10 mL) was stirred under hydrogen at 2.7 atm for 7 h. The catalyst was removed by filtration through diatomaceous earth, the solvent removed from the filtrate by evaporation and the solid residue washed with ether, collected by filtration, and dried under vacuum to give 930 mg of **67** (91%). ¹H NMR: δ 2.22 (s, 3H, CH₃CO), 3.87 (s, 3H, CH₃O), 4.02 (s, 3H, CH₃O), 6.9 (s, 1H, H8), 7.4–7.5 (m, 2H, H3' and H6'), 7.99 (s, 1H, H5), 8.62 (s, 1H, H2). MS—ESI m/z 372 [MH]⁺.

N-(2-Fluoro-5-methoxycarbonyloxy-4-methylphenyl)-6-methoxy-7-methoxyacetamido-4-quinazolinylamine 68. Methoxyacetyl chloride (62 μ L, 0.68 mmol) was added dropwise to a solution of *N*-7-amino-(2-fluoro-5-methoxycarbonyloxy-4-methylphenyl)-6-methoxy-4-quinazolinylamine hydrochloride **67** (215 mg, 0.52 mmol) in methylene chloride (5 mL) and pyridine (1.5 mL) at 0 °C and the mixture stirred for 2 h at 0 °C. Further methoxyacetyl chloride (14 μ L, 0.15 mmol) was added and the mixture stirred for further 20 min at 0 °C. The reaction mixture was partitioned between ethyl acetate and water and the aqueous layer adjusted to pH = 9 with saturated aqueous sodium bicarbonate solution. The organic layer was separated, washed with brine, dried (MgSO₄) and the solvent removed by evaporation. The residue was purified by column chromatography eluting with methylene chloride/acetonitrile/methanol (60:38:2) to give 175 mg of **68** (75%). ¹H NMR: δ 2.21 (s, 3H, CH₃CO), 3.47 (s, 3H, CH₃O), 3.87 (s, 2H, CH₂O), 4.07 (s, 3H, CH₃O), 4.15 (s, 3H, CH₃O), 7.35 (d, 1H, H3'), 7.45 (d, 1H, H6'), 7.96 (s, 1H, H8), 8.40 (s, 1H, H5), 8.65 (s, 1H, H2), 9.28 (s, 1H, NH), 9.65 (s, 1H, NH).

7-Fluoro-3,4-dihydroquinazolin-4-one 69. A solution of 2-amino-4-fluorobenzoic acid (3 g, 19.3 mmol) in formamide (30 mL) was heated at 150 °C for 6 h. The reaction mixture was poured onto ice–water (1:1) (250 mL). The precipitated solid was collected by filtration, washed with water, and dried to give 2.6 g of **69**²⁷ (82%). ¹H NMR (DMSO-*d*₆, CF₃COOD): δ 7.42 (m, 1H, H6), 7.48 (dd, 1H, H8), 8.22, (dd, 1H, H5), 8.4 (s, 1H, H2). MS—EI m/z 164 [M]⁺. Anal. (C₈H₅FN₂O) C, H, N.

7-(2-Methoxyethoxy)-3,4-dihydroquinazolin-4-one 70. Sodium (400 mg, 17 mmol) was added carefully to 2-methoxyethanol (10 mL) and the mixture heated at reflux for 30 min. 7-Fluoro-3,4-dihydroquinazolin-4-one **69**²⁷ (750 mg, 4.57 mmol) was added to the resulting solution and the mixture heated at reflux for 15 h. The mixture was cooled and poured into water (250 mL). The mixture was acidified to pH = 4 with concentrated hydrochloric acid. The resulting solid product was collected by filtration, washed with water and then with ether, and dried under vacuum to give 580 mg of **70** (58%). ¹H NMR (DMSO-*d*₆, CF₃COOD): δ 3.95 (s, 3H, CH₃O), 4.4 (t, 2H, CH₂O), 4.95 (t, 2H, CH₂O), 7.85 (d, 1H, H8), 7.95 (dd, 1H, H6), 8.75 (d, 1H, H5), 9.62 (s, 1H, H2). MS—EI m/z 220 [M]⁺. Anal. (C₁₁H₁₂N₂O₃) C, H, N.

5-Methoxy-4-(2-methoxyethoxy)-2-nitroacetophenone 75. 3-Methoxy-4-(2-methoxyethoxy)acetophenone **74** (18.1 g, 80 mmol) was added in portions over 50 min to a solution of nitric acid (163 mL, 69.5%) and cooled to 2 °C. After the solution was stirred for 2 h at ambient temperature, the reaction mixture was poured onto ice and extracted with ethyl acetate. The organic layer was washed with water and brine, dried (MgSO₄), and the solvent evaporated. The residue was purified by flash chromatography using methylene chloride/ethyl acetate (95:5) as eluent to give 17.4 g of **75** (80%). Mp 120–124 °C. ¹H NMR (CDCl₃): δ 2.5 (s, 3H, CH₃CO), 3.45 (s, 3H, CH₃OCH₂), 3.8 (t, 2H, CH₂OCH₃), 3.95 (s, 3H, CH₃O), 4.25 (t, 2H, CH₂OAr), 6.75 (s, 1H, H6), 7.7 (s, 1H, H3). ¹³C NMR: δ 29.9 (CO—CH₃), 56.6 (Ph—O—CH₃), 58.1 (CH₂—O—CH₃), 68.4 (Ph—O—CH₂), 69.9 (CH₃—O—CH₂), 108.1 (C8), 109.8 (C5), 131.2 (C10), 138.3 (C9), 148.5 (C6 or C7), 153.2 (C7 or C6), 199.3 (C=O). MS—EI m/z 269 [M]⁺. Anal. (C₁₂H₁₅NO₆) C, H, N.

2-Amino-5-methoxy-4-(2-methoxyethoxy)acetophenone 76. Iron powder (10 g, 180 mmol) was added in portions to a solution of 2-nitro-4-(2-methoxyethoxy)-5-methoxyacetophenone **75** (17.3 g, 64 mmol) in acetic acid (80 mL) and heated at 100 °C. After the solution was stirred for 30 min at 100 °C, the mixture was cooled and water (20 mL) was added. The mixture was extracted with ethyl acetate, the combined extracts were washed with water, saturated sodium carbonate solution, and brine and then dried (MgSO₄), and the solvent was evaporated. The residue was purified by flash chromatography using methylene chloride/ethyl acetate (8:2 followed by 75:25) as eluent to give 12.52 g of **76** (81%). Mp 99–101 °C. ¹H NMR (CDCl₃): δ 2.52 (s, 3H, CH₃CO), 3.45 (s, 3H, CH₃OCH₂), 3.8 (t, 2H, CH₂O), 3.85 (s, 3H, CH₃O), 4.15 (t, 2H,

CH₂O), 6.12 (s, 1H), 6.22 (bs, 1H), 7.12 (s, 1H). MS—EI *m/z* 239 [M]⁺. Anal. (C₁₂H₁₇NO₄) C, H, N.

6-Methoxy-7-(2-methoxyethoxy)-1,4-dihydroquinolin-4-one 77. A mixture of 4-methoxy-3-(2-methoxyethoxy)aniline **81** (5 g, 25.3 mmol) and diethylethoxymethylenemalonate (6 mL, 30 mmol) was heated at 110 °C for 30 min. Diphenyl ether (5 mL) was added and the mixture was heated at 240 °C for 6 h. The mixture was allowed to cool and diluted with petroleum ether. The resulting solid was collected by filtration and purified by reverse phase chromatography on a Diaion (trade mark of Mitsubishi) HP20SS resin column eluting with acetonitrile/water (40:60) to give 500 mg of **77** (8%). ¹H NMR: δ 3.35 (s, 3H, CH₃O), 3.75 (dd, 2H, CH₂O), 3.85 (s, 3H, CH₃O—Ph), 4.18 (dd, 2H, CH₂O), 5.95 (d, 1H, H₂), 7.0 (s, 1H, H₅), 7.48 (s, 1H, H₈), 7.78 (d, 1H, H₃). ¹³C NMR: δ 55.4 (Ph—O—CH₃), 58.2 (CH₂—O—CH₃), 67.7 (Ph—O—CH₂), 70.0 (CH₃—O—CH₂), 100.0 (C₈), 104.3 (C₅), 107.7 (C₁₀), 119.8 (C₁₀), 137.9 (C₂), 146.5 (C₆), 151.9 (C₇), 175.6 (C₄). MS—ESI *m/z* 250 [MH]⁺.

4-Methoxy-3-(2-methoxyethoxy)nitrobenzene 80. A mixture of 2-methoxy-5-nitrophenol **79** (6 g, 35 mmol), 2-bromoethyl methyl ether (4 mL, 40 mmol), potassium carbonate (5.8 g, 40 mmol), and potassium iodide (0.5 g) in DMF (50 mL) was heated at 80 °C for 1 h. The mixture was allowed to cool and then poured into water (400 mL). The resulting precipitate was collected by filtration, washed with water, and dried under vacuum to give 7.75 g of **80** (98%). ¹H NMR (CDCl₃): δ 3.46 (s, 3H, CH₃O), 3.82 (t, 2H, CH₂O), 3.96 (s, 3H, CH₃O—Ph), 4.25 (t, 2H, CH₂O), 6.91 (d, 1H, H₅), 7.79 (d, 1H, H₂), 7.92 (dd, 1H, H₆). ¹³C NMR: δ 56.2 (Ph—O—CH₃), 58.1 (CH₂—O—CH₃), 68.1 (Ph—O—CH₂), 70.1 (CH₂—O—CH₃), 107.3 (C₈), 111.0 (C₅), 117.7 (C₁₀), 140.6 (C₉), 147.7 (C₇), 154.7 (C₆). MS—ESI *m/z* 227 [MH]⁺.

4-Methoxy-3-(2-methoxyethoxy)aniline 81. A mixture of 4-methoxy-3-(2-methoxyethoxy)nitrobenzene **80** (7 g, 30 mmol) and 10% palladium on charcoal catalyst (1.4 g) in ethyl acetate (70 mL) was stirred under hydrogen at 3.3 atm pressure for 1 h. The catalyst was removed by filtration through diatomaceous earth and the solvent removed by evaporation. The solid residue was suspended in ethyl acetate, collected by filtration, and dried under vacuum to give 6.1 g of **81** (100%). ¹H NMR (CDCl₃): δ 3.4 (s, 3H, CH₃O), 3.75 (t, 2H, CH₂O), 3.8 (s, 3H, CH₃O—Ph), 4.12 (t, 2H, CH₂O), 6.24 (dd, 1H, H₆), 6.34 (d, 1H, H₂), 6.7 (d, 1H, H₅). ¹³C NMR: δ 56.6 (Ph—O—CH₃), 58.1 (CH₂—O—CH₃), 67.3 (Ph—O—CH₂), 70.4 (CH₂—O—CH₃), 101.1 (C₈), 105.5 (C₁₀), 114.9 (C₅), 140.2 (C₉), 143.3 (C₇), 148.9 (C₆). MS—ESI *m/z* 197 [MH]⁺.

4-Hydroxy-6-methoxy-7-(2-methoxyethoxy)cinnoline 82. A solution of sodium nitrite (3.9 g, 56 mmol) in water (5 mL) was added dropwise, to a solution of 2-amino-5-methoxy-4-(2-methoxyethoxy)acetophenone **76** (12.18 g, 50 mmol) in acetic acid (180 mL) and sulfuric acid (30 mL). After the solution was stirred for 90 min at 80 °C, the solution was concentrated to half its original volume and poured into ether (800 mL). The solid was collected by filtration and suspended in water (400 mL). After the pH was adjusted to 7.6 with 2 N aqueous sodium hydroxide solution, the solid was filtered off and washed with ether to give 8 g of **82** (62%). Mp 232–234 °C. ¹H NMR (DMSO-*d*₆, CF₃COOD): δ 3.35 (s, 3H, CH₃O), 3.75 (t, 2H, CH₂OCH₃), 3.9 (s, 3H, CH₃O), 4.2 (t, 2H, CH₂OAr), 6.95 (s, 1H, H₃), 7.35 (s, 1H, H₈), 7.65 (s, 1H, H₅). ¹³C NMR: δ 55.7 (Ph—O—CH₃), 58.2 (CH₂—O—CH₃), 67.9 (Ph—O—CH₂), 69.9 (CH₃—O—CH₂), 97.1 (C₈), 102.1 (C₅), 117.8 (C₁₀), 137.4 (C₆), 138.9 (C₃), 148.3 (C₉), 153.8 (C₇), 168.5 (C₄). MS—EI *m/z* 250 [M]⁺. Anal. (C₁₂H₁₄N₂O₄) C, H, N.

4-Chloro-6-methoxy-7-(2-methoxyethoxy)cinnoline 83. A solution of 4-hydroxy-6-methoxy-7-(2-methoxyethoxy)cinnoline **82** (7.8 g, 31 mmol) in thionyl chloride (130 mL) containing DMF (0.8 mL) was stirred at 80 °C for 2 h. After dilution with toluene, the mixture was evaporated to dryness. The resulting solid was filtered off, washed with ether, and then dissolved in ethyl acetate. The ethyl acetate solution was washed with saturated aqueous sodium bicarbonate solution, brine, dried

(MgSO₄), and the solvent evaporated. The residue was purified by flash chromatography using methylene chloride/ethyl acetate (1:9) as eluent to give 6.2 g of **83** (74%). Mp 171–173 °C. ¹H NMR (CDCl₃): δ 3.52 (s, 3H, CH₃OCH₂), 3.9 (t, 2H, CH₂—OCH₃), 4.1 (s, 3H, OCH₃), 4.4 (s, 2H, CH₂OAr), 7.75 (s, 1H, H₅), 7.23 (s, 1H, H₈), 9.15 (s, 1H, H₃). ¹³C NMR: δ 56.5 (CH₃O), 58.2 (CH₂OCH₃), 68.4 (PhCH₂O), 69.9 (CH₃OCH₂), 99.1 (C₈), 107.2 (C₅), 121.0 (C₄), 131.3 (C₁₀), 143.1 (C₃), 148.4 (C₉), 153.0 (C₆ or C₇), 154.6 (C₆ or C₄). MS—EI *m/z* 268 [M]⁺. Anal. (C₁₂H₁₃N₂O₃Cl) C, H, N.

4-Fluoro-2-methylphenyl methyl carbonate 84. Methyl chloroformate (6.8 mL, 88 mmol) was added over 30 min to a solution of 4-fluoro-2-methylphenol (10 g, 79 mmol) in 6% aqueous sodium hydroxide solution at 0 °C. The mixture was stirred for 2 h, then extracted with ethyl acetate (100 mL). The ethyl acetate extract was washed with water (100 mL) and dried (MgSO₄) and the solvent removed by evaporation to give 11.4 g of **84** (78%). ¹H NMR: δ 2.14 (s, 3H, CH₃), 3.81 (s, 3H, CH₃O), 7.05 (m, 1H), 7.1–7.25 (m, 2H).

4-Fluoro-2-methyl-5-nitrophenol 85. A mixture of concentrated nitric acid (6 mL) and concentrated sulfuric acid (6 mL) was added slowly to a solution of 4-fluoro-2-methylphenyl methyl carbonate **84** (11.34 g, 62 mmol) in concentrated sulfuric acid (6 mL) such that the temperature of the mixture was kept below 50 °C. The mixture was stirred for 2 h, added to ice–water (1:1) and the precipitated product collected by filtration. The crude product was purified by chromatography on silica eluting with methylene chloride/hexane progressing through increasingly polar mixtures to methanol/methylene chloride (1:19) to give 2.5 g of **85** (22%). ¹H NMR (DMSO-*d*₆, CD₃COOD): δ 2.31 (s, 3H, CH₃), 7.38 (d, 1H, H₃), 7.58 (d, 1H, H₆). MS—ESI *m/z* 171 [MH]⁺.

2-Fluoro-5-hydroxy-4-methylaniline 86. A mixture of 4-fluoro-2-methyl-5-nitrophenol **85** (2.1 g, 13 mmol), iron powder (1 g, 18 mmol) and iron(II)sulfate (1.5 g, 10 mmol) in water (40 mL) was heated at reflux for 4 h. The mixture was allowed to cool, neutralized with 2 N aqueous sodium hydroxide, and extracted with ethyl acetate (100 mL). The ethyl acetate extract was dried (MgSO₄) and the solvent removed by evaporation to give 0.8 g of **86** (47%). ¹H NMR: δ 1.94 (s, 3H, CH₃), 4.67 (s, 2H, NH₂), 6.22 (d, 1H, H₃ or H₆), 6.65 (d, 1H, H₃ or H₆), 8.68 (s, 1H, OH). MS—ESI *m/z* 142 [MH]⁺.

2-Chloro-4-fluoro-methoxycarbonyloxybenzene 87. To a solution of 0.5 N aqueous sodium hydroxide cooled at 5 °C was added 2-chloro-4-fluorophenol (29.3 g, 0.2 mol), followed by dropwise addition of methylchloroformate (23.6 g, 0.25 mol), while keeping the temperature below 5–10 °C. After the solution was stirred for 15 min at this temperature, the solid was filtered, washed with water and dried under vacuum to give 40.5 g of **87** (99%). Mp 73–74 °C. ¹H NMR (CDCl₃): δ 3.9 (s, 3H, CH₃O), 7.05 (dt, 1H, H₆), 7.2 (m, 2H, H₅ and H₃). MS—EI *m/z* 204 [M]⁺. Anal. (C₈H₆ClFO₃) C, H.

2-Chloro-4-fluoro-5-nitro-methoxycarbonyloxybenzene 88. To a suspension of 2-chloro-4-fluoro-methoxycarbonyloxybenzene **87** (40 g, 0.2 mol) in concentrated sulfuric acid (15 mL) was added a mixture of sulfuric acid (15 mL) and nitric acid 70% (15 mL), dropwise to keep the temperature below 30 °C. The mixture was stirred for 30 min at this temperature after completion of the addition. The mixture was poured onto a mixture of ice–water. The orange solid was filtered, washed with water, and dried under vacuum. The solid was dissolved in ether and the ethereal solution was washed with water, brine, dried (MgSO₄), filtered, and evaporated to give 41 g of **88** (82%). Mp 59–60 °C. ¹H NMR (CDCl₃): δ 3.98 (s, 3H, CH₃O), 7.45 (d, 1H, H₃), 8.05 (d, 1H, H₆). MS—EI *m/z* 249 [M]⁺. Anal. (C₈H₅ClFNO₅) C, H, N.

5-Amino-2-chloro-4-fluoro-methoxycarbonyloxybenzene 89. A solution of 2-chloro-4-fluoro-5-nitro-methoxycarbonyloxybenzene **88** (20 g, 80 mmol) in ethanol (300 mL) containing platinum oxide (200 mg) was hydrogenated for 3 h and ethyl acetate (200 mL) was added. Hydrogenation was continued for 2 h, and the mixture was filtered. The solvent was removed by evaporation and the oily residue triturated with ether. The resulting solid was filtered, washed with ether,

and dried under vacuum to give 15 g of **89** (82%). Mp 85–86 °C. ¹H NMR (CDCl₃): δ 3.92 (s, 3H, CH₃O), 6.63 (d, 1H, H6), 7.08 (d, 1H, H3). MS–EI *m/z* 219 [M]⁺. Anal. (C₈H₇ClFNO₃) C, H, N.

2-[N-Methyl-N-(4-pyridyl)]aminoethanol 90. A solution of 4-chloropyridine hydrochloride (4.5 g, 30 mmol) and 1-methyl-1-(hydroxyethyl)amine (2.25 g, 30 mmol) in 3-methyl-1-butanol (50 mL) containing NaHCO₃ (7.56 g, 90 mmol) was refluxed for 2 days. After removal of the solvent under vacuum, the residue was triturated with ethyl acetate. The solid was filtered off and washed with more ethyl acetate. The ethyl acetate layers were combined and evaporated. The resulting brown oil was purified by chromatography on neutral alumina eluting with methylene chloride–methanol (96:4) to give 300 mg of **90** (6%). Mp 87–88 °C. ¹H NMR (CDCl₃): δ 3.05 (s, 3H, NCH₃), 3.53 (t, 2H, CH₂OH), 3.83 (t, 2H, CH₂N), 6.5 (d, 2H, pyridine C=CH), 8.15 (d, 2H, pyridine CH=N–CH). MS–EI *m/z* 152 [M]⁺. Anal. (C₈H₁₂N₂O·0.1 MeOH) C, H, N.

Biological Evaluation. IC₅₀ reported are average figures of 3 to 5 measurements, depending on the compound potency.

(a) In Vitro Receptor Tyrosine Kinase Inhibition Test. This assay determined the ability of a test compound to inhibit tyrosine kinase activity.

Flt-1 (Genbank accession number × 51602), KDR (Genbank accession number L04947), and FGFR1 (Genbank accession number × 51803) cytoplasmic domains (2, 16, and 2 amino acids after the transmembrane region to the C-terminus, respectively), were isolated by PCR from a human placental cDNA library (Clontech Cat no. HL1008b). In each case, a methionine codon was added to the 5'-end, and coding regions were flanked by *Bam*H1 restriction sites to enable cloning into the baculovirus expression vector pACYM1. Recombinant proteins were expressed in *Spodoptera frugiperda* 21 (Sf 21) insect cells. For KDR and FGFR1 receptor tyrosine kinases, 3 × 10⁷ Sf21 cells were infected with plaque-pure recombinant virus at a multiplicity of infection of 3 (175 cm³ flask). Flt-1 expression was achieved by infecting 2 × 10⁶ Sf9 insect cells at a multiplicity of infection of 1 (5 L bioreactor). Cells were harvested after 48 h, washed with ice cold phosphate buffered saline (PBS), and resuspended in an ice cold HNTG/PMSF solution (20 mM Hepes, pH 7.5, 150 mM sodium chloride, 10% v/v glycerol, 1% v/v Triton × 100, 1.5 mM magnesium chloride, 1 mM ethylene glycol–bis(baminoethyl ether) *N,N,N,N*-tetraacetic acid (EGTA), and 1 mM phenylmethylsulfonyl fluoride (PMSF)), using 1 mL of HNTG/PMSF per 10⁶ cells. The suspension was centrifuged for 10 min at 13 000 rpm at 4 °C, and the supernatant (enzyme stock) removed and stored in aliquots at –70 °C. Each new batch of stock enzyme was titrated in the assay following dilution with enzyme diluent (100 mM Hepes pH 7.4, 0.2 mM Na₃VO₄, 0.1% v/v Triton × 100, 0.2 mM DTT). For a typical batch, stock enzyme was diluted 1 in 2000 with enzyme diluent and 50 μL of dilute enzyme used per well.

A poly(glu, ala, tyr) 6:3:1 random copolymer (Sigma, Poole, UK) was used as a tyrosine containing substrate solution. The substrate was stored as a 1 mg/mL stock in PBS at –20 °C and diluted 1 in 500 with PBS in order to coat 96 well plates (100 μL/well). Plates were coated on the day prior to assay, sealed with adhesive seals, and stored overnight at 4 °C. On the day of the assay, the substrate solution was discarded and the assay plate wells were washed once with PBST (PBS containing 0.05% v/v Tween 20) and once with Hepes buffer (50 mM, pH 7.4).

Test compounds were diluted with 10% dimethylsulfoxide (DMSO) de-ionized water and 25 μL volumes transferred to wells in the washed assay plates. Manganese chloride solution (40 mM) containing 8 μM ATP was then added (25 μL) to all test wells. Control and blank wells, containing compound diluent and manganese chloride solution with and without ATP, respectively, were also included to determine the dynamic range of the assay. Freshly diluted enzyme (50 μL) was added to each well, and the plates incubated at room temperature for 20 min. The liquid was then discarded and the wells were washed twice with PBST. Mouse IgG anti-phosphoty-

rosine antibody (Upstate Biotechnology Inc., Lake Placid, USA) diluted 1:6000 with PBST containing 0.5% (w/v) bovine serum albumin (BSA) was added (100 μL/well), and the plates incubated for 1 h at room temperature before discarding the liquid and washing the wells twice with PBST. Horseradish peroxidase (HRP)-linked sheep anti-mouse Ig antibody (Amersham, Little Chalfont, UK) diluted 1:500 with PBST containing 0.5% (w/v) BSA, was then added (100 μL/well) and the plates incubated for a further 1 h at room temperature before discarding the liquid and washing the wells twice with PBST. A 1 mg/mL solution of 2,2'-azino-bis(3-ethylbenzthiazoline-6-sulfonic acid (Boehringer, Lewes, UK) was freshly prepared in 50 mM phosphate-citrate buffer (pH5.0) containing 0.03% (w/v) sodium perborate, and 100 μL added to each well. Plates were then incubated for 20–60 min at room temperature until the optical density value of control wells measured at 405 nm was approximately 1.0. IC₅₀ values for compound enzyme inhibition were interpolated using Microcal Origin following subtraction of blank values.

The exact enzyme concentration of the different preparations of partially purified enzyme isolated from the insect cell lysate is not known. The precise state of phosphorylation of these partially purified enzymes is also unknown. However, the degree of phosphorylation of several batches of enzyme protein, prepared by the method described, was checked by western blotting, using anti-phosphotyrosine antibody, and this did not appear to grossly influence the activity of the enzyme.

(b) In Vitro HUVEC Proliferation Assay. HUVEC cells were isolated in MCDB 131 (Gibco BRL) + 7.5% v/v foetal calf serum (FCS) and were plated out (at passage 2 to 8), in MCDB 131 + 2% v/v FCS + 3 μg/mL heparin + 1 μg/mL hydrocortisone, at a concentration of 1000 cells/well in 96 well plates. After a minimum of 4 h they were dosed with the appropriate growth factor (i.e., VEGF₁₆₅ 3 ng/mL or b-FGF 0.3ng/mL) and compound. The cultures were then incubated for 4 days at 37 °C with 7.5% CO₂. On day 4, the cultures were pulsed with 1 μCi/well of tritiated thymidine (Amersham product TRA 61) and incubated for 4 h. The cells were harvested using a 96-well plate harvester (Tomtek) and then assayed for incorporation of tritium with a Beta plate counter. Incorporation of radioactivity into cells, expressed as cpm, was used to measure inhibition of growth factor-stimulated cell proliferation by compounds.

(c) In Vivo Rat Uterine Oedema Assay. The assay was performed in groups of newly weaned, 20- to 22-day old female rats. One group received dosing vehicles only and served as the "untreated" controls. All other groups were treated with a single subcutaneous dose of oestradiol benzoate (2.5 μg/rat) in arachis oil. One group received only this treatment and served as the "oestrogen alone" controls. To the remaining groups, test compounds were administered orally 18 h and 1 h prior to the administration of oestradiol benzoate. The compounds were administered as ball-milled suspensions in 0.1% aqueous polysorbate 80. Five hours after the administration of oestradiol benzoate, the rats were humanely killed and their uteri were dissected, blotted, and weighed. The increase in uterine weight in groups treated with test compound and oestradiol benzoate and with oestradiol benzoate alone was compared using a Student T test. Inhibition of the effect of oestradiol benzoate was considered significant when *p* < 0.05.

The VEGF m-Ab used as VEGF scavenger in the uterine oedema assay was purchased from R&D Systems.

(d) Mouse Strain and Dosing Methodology. Female Swiss mice were used in plasma pharmacokinetic studies, while tumor xenograft experiments used female athymic (nu/nu genotype) Swiss mice maintained in negative pressure isolators (PFI Systems Ltd, Oxon, UK). Mice were bred at Alderley Park, housed in a barrier facility with 12 h light/dark cycles and provided with sterilized food and water ad libitum. All procedures were performed on mice of at least 8 weeks of age, within a weight range of 27–35 g. In all studies, compounds were suspended in a 1% (v/v) solution of polyoxy-

ethylene (20) sorbitan mono-oleate in distilled water, and dosed by oral gavage at 0.1 mL/10 g body weight.

(e) Plasma Pharmacokinetic Assay. Unless specified, all reagents were of Analar or HPLC grade and obtained from Fisher Scientific Ltd. (Loughborough, UK). Compounds were administered to groups of three mice, and blood collected 6 h after dosing by pooling samples containing a given compound into a 1.5 mL lithium heparin tube. Samples were immediately centrifuged (16000g, 10 min), plasma removed by aspiration into 1.5 mL microcentrifuge tubes, and duplicate 200 μ L aliquots removed for analysis. Additional plasma aliquots containing either no compound (as a control), or a series of compound standards (seriallyly diluted 1:2 to give a range from 5.8 to 0.09 μ M) were also prepared in duplicate. Acetonitrile (400 μ L) was added to each sample aliquot, while gently vortexing to precipitate plasma protein. Following additional vortexing (15 s) tubes were centrifuged (16000g, 30 s), and 550 μ L of supernatant removed and diluted with deionized water (250 μ L).

Plasma concentrations were determined by reverse-phase HPLC with UV detection. Samples were analyzed using a Constametric 3000 pump and a Spectromonitor D variable wavelength UV detector (LDC Milton Roy, Staffs, UK), with an ISS-101 autosampler (Perkin-Elmer, Uberlign, Germany). Pump control and data acquisition were performed using EZ Chrom Chromatography software (Version 6.6, Scientific Software Inc., San Ramon, CA) and chromatographic separation achieved using a Columbus C18 analytical column (3 μ m; 100 \times 4.6 mm I.D.), preceded by a Columbus C18 guard cartridge (3 μ m; 10 \times 3.2 mm I.D.) (Phenomenex Ltd., Macclesfield, UK). A mobile phase of 70% (v/v) methanol in 0.1 M ammonium acetate (prepared in double distilled water) was degassed with a stream of helium (15 min) prior to use. Samples (150 μ L injection volume) were eluted isocratically at a flow rate of 1 mL/min, under ambient temperature, and compounds detected within a wavelength range of 335–340 nm. Calibration curves were constructed using peak height and concentrations of unknowns interpolated accordingly. Results were reported as the mean of duplicate samples.

(f) Human Tumor Xenograft Test. The human lung carcinoma cell line Calu-6 was obtained from the American Type Culture Collection (Manassas, VA). All cell culture reagents, unless otherwise specified, were obtained from Life Technologies, Paisley, UK). Cells were maintained as an exponentially growing monolayer in Minimal Essential Medium with Earles' salts, supplemented with 1 mM sodium pyruvate, 1% nonessential amino acids, 10% FCS (Labtech International, Ringmer, UK) and 2 mM L-glutamine (Sigma Chemical Co., Poole, UK). The cell line was found to be negative for microplasma in culture, and for 15 types of virus when screened in a mouse antibody production test (Central Toxicology Laboratories, Alderley Park, UK) prior to routine use in vivo.

Calu-6 tumor xenografts were established in the hind flank of mice by s.c. injection of 1×10^6 cells, in 100 μ L of 50% (v/v) Matrigel (Fred Baker, Liverpool, UK) in serum free media. Ten days after cell implantation, mice were divided into groups with tumor sizes ranging from 0.33 to 0.54 cm³, and received either compound or vehicle once daily for 21 days. Tumor volume was assessed twice weekly by bilateral vernier caliper measurement, using the formula (length \times width) \times $\sqrt{(\text{length} \times \text{width})} \times (\pi/6)$, where length was the longest diameter across the tumor and width the corresponding perpendicular. Growth inhibition from the start of treatment was calculated by comparison of the mean change in tumor volume for the control and treated group, and statistical significance evaluated using a one-tailed t-test.

Acknowledgment. The technical assistance of Janet Jackson, Brenda Currie, Cath Grundy, Claire Barnes, Jodie Sharpless, Rosemary Chester Philip, Tina Hayden, Sarah Boffey, Karen Malbon, Paula Valentine, Jonathan Mills, Dick Glarvey, Janet Culshaw, Glynn Chesterton, Steve Glossop, Scott Lamont, David Milnes,

Georges Pasquet, Patrice Koza, Myriam Didelot, Dominique Boucherot, Pascal Boutron, Françoise Magnien, and Christian Delvare is gratefully acknowledged. We also thank Phil Jewsbury for his help in building the Flt1 3D model.

Supporting Information Available: The complete experimental procedures for the synthesis of **3–10, 12, 14, 17–19, 21, 22, 25, 26, 28, 30, 35, 41, 43–45, 48, 49, 54, 56–58, 63–65, 71, 72, 74, 78**. This material is available free of charge via the Internet at <http://pubs.acs.org>.

References

- Fan, T. P. D.; Jaggar, R.; Bicknell, R. Controlling the vasculature: angiogenesis, anti-angiogenesis, and vascular targeting of gene therapy. *Trends Pharmacol. Sci.* **1995**, *16*, 57–66.
- Folkman, J. Angiogenesis in cancer, vascular, rheumatoid and other disease. *Nature Medicine* **1995**, *1*, 27–31.
- Cullinan-Bove, K.; Koos, R. D. Vascular endothelial growth factor/vascular permeability factor expression in the rat uterus: Rapid stimulation by estrogen correlates with estrogen-induced increases in uterine capillary permeability and growth. *Endocrinology* **1993**, *133*, 829–837.
- Senger, D. R.; Van De Water, L.; Brown, L. F.; Nagy, J. A.; Yeo, K. T.; Yeo, T. K.; Berse, B.; Jackman, R. W.; Dvorak, A. M.; Dvorak, H. F. Vascular permeability factor (VPF, VEGF) in tumor biology. *Cancer and Metastasis Reviews* **1993**, *12*, 303–324.
- Hanahan, D.; Folkman, J. Patterns and emerging mechanisms of the angiogenic switch during tumorigenesis. *Cell* **1996**, *86*, 353–364.
- Jakeman, L. B.; Armanini, M.; Phillips, H. S.; Ferrara, N. Developmental expression of binding sites and messenger ribonucleic acid for vascular endothelial growth factor suggests a role for this protein in vasculogenesis and angiogenesis. *Endocrinology* **1993**, *133*, 848–859.
- Connolly, D. T.; Olander, J. V.; Heuvelman, D.; Nelson, R.; Monsell, R.; Siegel, N.; Haymore, B. L.; Leimgruber, R.; Feder, J. Human vascular permeability factor. Isolation from U937 cells. *J. Biol. Chem.* **1989**, *264*, 20017–20024.
- Plowman, G. D.; Ullrich, A.; Shawver, L. K. Receptor tyrosine kinases as targets for drug intervention. *Drug News Perspect.* **1994**, *7*, 334–339.
- Straw, L. M.; Shawver, L. K. Tyrosine kinases in disease: overview of kinase inhibitors as therapeutic agents and current drugs in clinical trials. *Exp. Opin. Invest. Drugs* **1998**, *7*, 553–573.
- Shawver, L. K.; Lipson, K. E.; Fong, T. A. T.; McMahon, G.; Plowman, G. D.; Strawn, L. M. Receptor tyrosine kinases as targets for inhibition of angiogenesis. *Drug Discov. Today* **1997**, *2*, 50–63.
- Tsai, J.-C.; Goldman, C. K.; Gillespie, G. Y. Vascular endothelial growth factor in human glioma cell lines: induced secretion by EGF, PDGF-BB, and bFGF. *J. Neurosurg.* **1995**, *82*, 864–873.
- Claffey, K. P.; Brown, L. F.; Del Aguila, L. F.; Tognazzi, K.; Manseau, E. J.; Dvorak, H. F. Expression of vascular permeability factor/vascular endothelial growth factor by melanoma cells increases tumour growth, angiogenesis, and experimental metastasis. *Cancer Res.* **1996**, *56*, 172–181.
- Anan, K.; Morosaki, T.; Katano, M. Vascular endothelial growth factor and platelet-derived growth factor are potential angiogenic and metastatic factors in human breast cancer. *Surgery* **1996**, *119*, 333–339.
- Yoshiji H.; Gomez D. E.; Shibuya, M.; Thorgeirsson, U. P. Expression of vascular endothelial growth factor, its receptor, and other angiogenic factors in human breast cancer. *Cancer Res.* **1996**, *56*, 2013–2016.
- Brown, L. F.; Berse, B.; Jackman, R. W.; Tognazzi, K.; Manseau, E. J.; Senger, D. R.; Dvorak, H. F. Expression of vascular permeability factor (vascular endothelial growth factor) and its receptors in adenocarcinomas of the gastrointestinal tract. *Cancer Res.* **1993**, *53*, 4727–4735.
- Takahashi, Y.; Kitadai, Y.; Bucana, C. D.; Cleary, K. R.; Ellis, L. M. Expression of vascular endothelial growth factor and its receptor, KDR correlates with vascularity, metastasis, and proliferation of human colon cancer. *Cancer Res.* **1995**, *55*, 3964–3968.
- Takahashi, A.; Sasaki, H.; Kim, S. J.; Tobisu, K.-I.; Kakizoe, T.; Tsukamoto, T.; Kumamoto, Y.; Sugimura, T.; Terada, M. Markedly increased amounts of messenger RNAs for vascular endothelial growth factor and placenta growth factor in renal cell carcinoma associated with angiogenesis. *Cancer Res.* **1994**, *54*, 4233–4237.
- Ullrich, A.; Schlessinger J. Signal transduction by receptor tyrosine kinase activity. *Cell* **1990**, *61*, 203–212.

- (19) Halaban, R. Growth factors and tyrosine protein kinases in normal and Malignant Melanocytes. *Cancer Met. Rev.* **1991**, *10*, 129–140.
- (20) Bishop, J. M. The Molecular genetic of cancer. *Science* **1987**, *335*, 305–311.
- (21) De Vries, C.; Escobedo, J. A.; Ueno, H.; Houck, K.; Ferrara, N.; Williams, L. T. The fms-like tyrosine kinase, a receptor for vascular endothelial growth factor. *Science* **1992**, *255*, 989–991.
- (22) Terman, B. I.; Dougher-Vermazen, M.; Carrion, M. E.; Dimitrov, D.; Armellino, D. C.; Gospodarowicz, D.; Bohlen, P. Identification of the KDR tyrosine kinase as a receptor for vascular endothelial cell growth factor. *Biochem. Biophys. Res. Comm.* **1992**, *187*, 1579–1586.
- (23) Kim, K. L.; Li, B.; Winer, J.; Armanini, M.; Gillett, N.; Phillips, H. S.; Ferrara, N. Inhibition of vascular endothelial growth factor-induced angiogenesis suppresses tumor growth in vivo. *Nature* **1993**, *362*, 841–844.
- (24) Sun, L.; Tran, N.; Tang, F.; App, H.; Hirth P.; McMahon G.; Tang, C. Synthesis and Biological Evaluation of 3-substituted Indolin-2-ones: A Novel Class of Tyrosine Kinase Inhibitors That Exhibit Selectivity toward Particular Receptor tyrosine Kinases. *J. Med. Chem.* **1998**, *41*, 2588–2603.
- (25) Bridges, A. J.; Zhou, H.; Cody, D. R.; Rewcastle, G. W.; McMichael, A.; Showalter, H. D.; Fry, D. W.; Kraker, A. J.; Denny, W. A. Tyrosine kinase inhibitors. 8. An unusually steep structure–activity relationship for analogues of 4-(3-bromoanilino)-6,7-dimethoxyquinazoline (PD 153035), a potent inhibitor of the epidermal growth factor receptor. *J. Med. Chem.* **1996**, *39*, 267–276.
- (26) Althuis, T. H.; Hess, H. J. Synthesis and Identification of the Major Metabolites of Prazosin in dog and Rat. *J. Med. Chem.* **1977**, *20*, 146–149.
- (27) Rewcastle, G. W.; Palmer, B. D.; Bridges, A. J.; Showalter, H. D.; Sun, L. Tyrosine kinase inhibitors. 9. Synthesis and evaluation of fused tricyclic quinazoline analogues as ATP site inhibitors of the tyrosine kinase activity of the epidermal growth factor receptor. *J. Med. Chem.* **1996**, *4*, 918–928.
- (28) Zeneca, unpublished data.
- (29) (a) Lohmann, J.-J. M.; Hennequin, L. F. A.; Thomas, A. P. Preparation and antiangiogenic and/or vascular permeability reducing effect of quinazoline derivatives. WO 9722596 A1 970626. CA:127:135808. (b) Thomas, A. P.; Hennequin, L. F. A.; Ple, P. A. Quinoline derivatives inhibiting the effect of growth factors such as VEGF. WO 9813350 A1 980402. CA:128:270546. (c) Thomas, A. P.; Hennequin, L. F. A.; Johnstone, C.; Stokes, E. S. E.; Lohmann, J.-J. M.; Clayton, E. Preparation of quinazoline derivatives and pharmaceutical compositions containing them. WO 9813354 A1 980402. CA:128:257441. (d) Thomas, A. P.; Hennequin, L. F. A. Preparation of anilinoquinolines and related compounds as inhibitors of angiogenesis and vascular permeability. WO 9734876 A1 970925. CA:127:307392. (e) Thomas, A. P.; Hennequin, L. F. A.; Johnstone, C. Preparation of 4-anilinoquinazolines for use in the treatment of disease states associated with antiangiogenesis and/or increased vascular permeability. WO 9732856 A1 970912. CA:127:278209. (f) Thomas, A. P.; Johnstone, C.; Hennequin, L. F. A. Preparation of quinazolines as VEGF inhibitors. WO 9730035 A1 970821. CA:127:262698.
- (30) Ward, W. H. J.; Cook, P. N.; Slater, A. M.; Davies, D. H.; Holdgate, G. A.; Green, L. R. Epidermal growth factor receptor tyrosine kinase. Investigation of catalytic mechanism, structure-based searching and discovery of a potent inhibitor. *Biochem. Pharmacol.* **1994**, *48*(4), 659–666.
- (31) Rewcastle, G. W.; Denny, W. A.; Bridges, A. J.; Zhou, H.; Cody, D. R.; McMichael, A.; Fry, D. W. Tyrosine kinase inhibitors. 5. Synthesis and structure–activity relationships for 4-[(phenylmethyl)amino]- and 4-(phenylamino)quinazolines as potent adenosine 5'-triphosphate binding site inhibitors of the tyrosine kinase domain of the epidermal growth factor receptor. *J. Med. Chem.* **1995**, *38*, 3482–3487.
- (32) Woodburn, A. J.; Barker, A. J.; Gibson, K. H.; Ashton, S. E.; Wakeling, A. E.; Curry, B. J.; Scarlett, L.; Henthorn, L. R. ZD1839, an epidermal growth factor tyrosine kinase inhibitor selected for clinical trial development. *Proc. Am. Assoc. Cancer Res.* **1997**, *38*, 6633 (Abstract 4251).
- (33) Gibson, K. H.; Grundy, W.; Godfrey, A. A.; Woodburn, J. R.; Ashton, S. E.; Curry, B. J.; Scarlett, L.; Barker, A. J.; Brown, D. S. Epidermal Growth Factor Receptor Tyrosine Kinase, Structure–Activity Relationship, and Antitumor Activity of Novel Quinazolines. *Biol. Med. Chem. Lett.* **1997**, *7*, 2723–2728.
- (34) Iwata, K.; Miller, P. E.; Barbacci, E. G.; Arnold, L.; Doty, J.; DiOrio, C. I.; Pustilnik, L. R.; Reynolds, M.; Theleman, A.; Sloan, D.; Moyer, J. D. CP-358,774: a selective EGFR kinase inhibitor with potent antiproliferative activity against HN5 head and neck tumor cells. *Proc. Am. Assoc. Cancer Res.* **1997**, *38*, 6633 (Abstract 4248).
- (35) Lamers, M. B. A. C.; Antson, A. A.; Hubbard, E. E.; Scott, R. K.; Williams, D. H. Structure of the protein tyrosine kinase domain of the C-terminal Src (CSK) in complex with Staurosporine. *J. Mol. Biol.* **1999**, *285*, 713–725.
- (36) Schulze-Gahmen, U.; Brandens, J.; Jones, H. D.; Morgan, D. O.; Meijer, L.; Vesely, J.; Kim, S. H. Multiple Modes of Ligand Recognition: Crystal Structures of Cyclin-Dependent Protein Kinase 2 in Complex with ATP and Two Inhibitors, Olomoucine and Isopentenyladenine. *Proteins: Struct., Funct., Genet.* **1995**, *22*, 378–391.
- (37) Schulze-Gahmen, U.; De Bondt, H. L.; Kim, S. H. High-resolution crystal structures of human cyclin-dependent kinase 2 with and without ATP: bound waters and natural ligand as guides for inhibitor design. *J. Med. Chem.* **1996**, *39*, 4540–4546.
- (38) Filgueira de Azevedo, Jr., W.; Mueller-Dieckmann, H.-J.; Schulze-Gahmen, U.; Worland, P. J.; Sausville, E.; Kim, S.-H. Structural basis for specificity and potency of a flavonoid inhibitor of human CDK2, a cell cycle kinase. *Proc. Natl. Acad. Sci. U.S.A.* **1996**, *93*, 2735–2740.
- (39) Lawrie, A. M.; Noble, M. E. M.; Tunnah, P.; Brown, N. R.; Johnson, L. N.; Endicott, J. A. Protein kinase inhibition by staurosporine revealed in details of the molecular interaction with CDK2. *Nature Struct. Biol.* **1997**, *4*(9), 796–800.
- (40) Engh, R. A.; Girod, A.; Kinzel, V.; Huber R.; Bossemeyer, D. Crystal structures of catalytic subunit of cAMP-dependent protein kinase in complex with isouinolinesulfonyl protein kinase inhibitors H7, H8, and H89. *J. Biol. Chem.* **1996**, *271*(42), 26157–26164.
- (41) Prade, L.; Engh, R. A.; Girod, A.; Kinzel, V.; Huber R.; Bossemeyer, D. Staurosporine-induced conformational changes of the cAMP-dependent protein kinase catalytic subunit explain inhibitory potential. *Structure* **1997**, *5*(12), 1627–1637.
- (42) Hubbard, S. Crystal structure of the activated insulin receptor tyrosine kinase in complex with peptide substrate and ATP analogue. *EMBO J.* **1997**, *16*, 5572–5581.
- (43) Sicheri, F.; Moarefi, I.; Kuriyan, J. Crystal structure of the Src family tyrosine kinase Hck. *Nature* **1997**, *385*, 602–609.
- (44) Mohamadi, M.; McMahon, G.; Sun, L. T.; Tang, C.; Hirth, P.; Yeh, B. K.; Hubbard, S. R.; Schlessinger, J. Structures of the tyrosine kinase domain of fibroblast growth factor receptor in complex with inhibitors. *Science* **1997**, *276*, 955–960.
- (45) Mohamadi, M.; Froum, S.; Hamby, J. M.; Schroeder, M. C.; Panek, R. L.; Lu, G. H.; Eliseenkova, A. V.; Green, D.; Schlessinger, J.; Hubbard, S. R. Crystal structure of an angiogenesis inhibitor bound to the FGF receptor tyrosine kinase domain. *EMBO J.* **1998**, *17*(20), 5896–5904.
- (46) Tong, L.; Pav, S.; White, D. M.; Rogers, S.; Crane, K. M.; Cywin, C. L.; Brown, M. L.; Pargellis, C. A. A highly specific inhibitor of human p38 MAP kinase binds in the ATP pocket. *Nature Struct. Biol.* **1997**, *4*(4), 311–316.
- (47) Wilson, K. P.; McCaffrey, P. G.; Hsiao, K.; Pazhanisamy, S.; Galullo, V.; Bemis, G. W.; Fitzgibbon, M. J.; Caron, P. R.; Murcko, M. A.; Su, M. S. S. The structural basis for the specificity of pyridinylimidazole inhibitors of p38 MAP kinase. *Chem. Biol.* **1997**, *4*, 423–431.
- (48) Furet, P.; Caravatti, G.; Priestle, J.; Sowadski, J.; Trinks, U.; Traxler, P. Modeling study of protein kinase inhibitors: binding mode of staurosporine and origin of the selectivity of CGP 52 411. *J. Comput.-Aided Mol. Des.* **1995**, *9*, 465–472.
- (49) Traxler, P. M.; Furet, P.; Mett, H.; Buchdunger, E.; Meyer, T.; Lydon, N. 4-(phenylamino)pyrrolopyrimidines: potent and selective, ATP site directed inhibitors of the EGF-receptor protein tyrosine kinase. *J. Med. Chem.* **1996**, *39*, 2285–2292.
- (50) Traxler, P. M.; Bold, G.; Frei, J.; Lang, M.; Lydon, N.; Mett, H.; Buchdunger, E.; Meyer, T.; Mueller, M.; Furet, P. Use of a Pharmacophore model for the design of EGF-R tyrosine kinase inhibitors: 4-(phenylamino)pyrazolo[3,4-d]pyrimidines. *J. Med. Chem.* **1997**, *40*, 3601–3616.
- (51) Palmer, B. D.; Trumpp-Kallmeyer, S.; Fry, D. W.; Nelson, J. M.; Showalter, H. D. H.; Denny, W. A. Tyrosine kinase inhibitors. 11. Soluble analogues of pyrrolo- and pyrazoloquinazolines as epidermal growth factor receptor inhibitors: synthesis, biological evaluation, and modeling of the mode of binding. *J. Med. Chem.* **1997**, *40*, 1519–1529.
- (52) Trumpp-Kallmeyer, S.; Rubin, J. R.; Humblet, C.; Hamby, J. M.; Showalter, H. D. H. Development of a Binding Model to Protein Tyrosine Kinases for Substituted Pyrido[2,3-d]pyrimidine Inhibitors. *J. Med. Chem.* **1998**, *41*, 1752–1763.
- (53) Zheng, J.; Trafny, E. A.; Knighton, D. R.; Xuong, N.-H.; Taylor, S. S.; Ten Eyck, L. F.; Sowadsky, J. M. 2.2 A refined crystal structure of the catalytic subunit of cAMP-dependent protein kinase complexed with MnATP and a peptide inhibitor. *Acta Crystallogr.* **1993**, *D49*, 362–365.
- (54) (a) Ogilvie, D. J.; Wedge, S. R.; Dukes, M.; Kendrew, J.; Curwen, J. O.; Thomas, A. P.; Hennequin, L. F.; Plé, P.; Stokes, E. S. E.; Johnstone, C.; Wadsworth, P.; Richmond, G. H. P.; Curry, B. ZD4190: An orally administered inhibitor of VEGF signaling with pan-xenograft anti-tumour activity. *AACR Philadelphia*

- 1999 Abstract 458. (b) Wedge, S. R.; Waterton, J. C.; Tessier, J. J.; Checkley, D.; Dukes, M.; Kendrew, J.; Curry, B. Effect of the VEGF receptor tyrosine kinase inhibitor ZD4190 on vascular endothelial permeability. *AACR Philadelphia* 1999 Abstract 2741. (To be published).
- (55) De Bondt, H. L.; Rosenblatt, J.; Jancarik, J.; Jones, H. D.; Morgan, D. O.; Kim, S. H. Crystal structure of cyclin-dependent kinase 2. *Nature* **1993**, *363*, 595–602.
- (56) Zang, F.; Strand, A.; Robbins, D.; Cobb, M. H.; Goldsmith, E. J. Atomic structure of the MAP kinase ERK2 at 2.3 Å resolution. *Nature* **1994**, *367*, 704–711.
- (57) Owen, D. J.; Noble, M. E. M.; Garman, E. F.; Papageorgiou, A. C.; Johnson, L. N. Two structures of the catalytic domain of phosphorylase kinase: an active protein kinase complexed with substrate analogue and product. *Structure* **1995**, *3*, 467–482.
- (58) Xu, R. M.; Carmel, G.; Sweet, R. M.; Kuret, J.; Cheng, X. Crystal structure of casein kinase-1, a phosphate-directed protein kinase. *EMBO J.* **1995**, *14*, 1015–1023.
- (59) (a) Hanks, S. K.; Quinn, A. M.; Hunter, T. The protein kinase family: conserved features and deduced phylogeny of the catalytic domains. *Science* **1988**, *241*, 42–52. (b) Hanks, S. K.; Quinn, A. M. Protein kinase catalytic domain sequence database: Identification of conserved features of primary structure and classification of family members. *Methods Enzymol.* **1991**, *200*, 38–62.
- (60) Zheng, J.; Knighton, D. R.; Xuong, N.-H.; Taylor, S. S.; Sowadsky, J. M.; Ten Eyck, L. F. Crystal structures of the myristylated catalytic subunit of cAMP-dependent protein kinase reveal open and closed conformations. *Protein Sci.* **1993**, *2*, 1559–1573.
- (61) Knighton, D. R.; Cadena, D. L.; Zheng, J.; Ten Eyck, L. F.; Taylor, S. S.; Sowadsky, J. M.; Gill, G. N. Structural features that specify tyrosine kinase activity deduced from homology modeling of the epidermal growth factor receptor. *Proc. Natl. Acad. Sci. U.S.A.* **1993**, *90*(11), 5001–5005.
- (62) Sali, A.; Blundell, T. L. Comparative protein modelling by satisfaction of spatial restraints. *J. Mol. Biol.* **1993**, *234*, 779–815.
- (63) Quanta; Molecular Simulations, Incorporated, 9685 Scranton Rd, San Diego, CA 92121-3752.
- (64) Brooks, B. R.; Brucoleri, R. E.; Olafson, B. D.; States, D. J.; Swaminathan, S.; Karplus, M. CHARMM: a program for macromolecular energy, minimisation, and dynamics calculations. *J. Comput. Chem.* **1983**, *4*, 187–217.
- (65) Momany, F. A.; Rone, R. Validation of the general purpose QUANTA3.2/CHARMM force field. *J. Comput. Chem.* **1992**, *13*, 888–900.
- (66) McTigue, M. A.; Wickersham, J. A.; Pinko, C.; Showalter, R. E.; Parast, C. V.; Tempczyk-Russel, A. T.; Gehring, M. R.; Mroczkowski, B.; Kan, C.-C.; Villafranca, J. E.; Appelt, K. Crystal structure of the kinase domain of human vascular endothelial growth factor receptor 2: a key enzyme in angiogenesis. *Structure* **1999**, *7*, 319–330.
- (67) Adams, R. R.; Whitmore, F. C. Heterocyclic basic compounds. IV. 2-aminoalkylamino-pyrimidines. *J. Am. Chem. Soc.* **1945**, *67*, 735–738.
- (68) Calderon, S. N.; Izenwasser, S.; Heller, B.; Gutkind, J. S.; Mattson, M. V., Su, T.-P.; Newman, A. H. Novel 1-Phenylcycloalkanecarboxylic Acid Derivatives Are Potent and Selective σ_1 Ligands. *J. Med. Chem.* **1994**, *37*, 2285–2291.
- (69) Yamaguchi, M.; Kamei, K.; Koga, T.; Akima, M.; Kuroki, T.; Ohi, N. Novel Antiasthmatic Agents with Dual Activities of Thromboxane A₂ Synthetase Inhibition and Bronchodilation. 1. 2-[2-(1-Imidazolyl)alkyl]-1(2H)-phthalazinones. *J. Med. Chem.* **1993**, *36*, 4052–4060.
- (70) Ainsworth, C.; Jones, R. G. Isomeric and Nuclear-substituted β -Aminoethyl-1,2,4-triazoles. *J. Am. Chem. Soc.* **1955**, *77*, 621–622.
- (71) Kume, M.; Kubota, T.; Kimura, Y.; Nakashimizu, H.; Motokawa, K.; Nakano M. Orally Active Cephalosporins II. Synthesis and Structure–Activity Relationships of New 7 β -[(Z)-2-(2-Aminothiazol-4-yl)-2-Hydroxyiminoacetamido]-Cephalosporins with 1,2,3-Triazole in C-3 Side Chain. *J. Antibio.* **1993**, *46*, 177–195.
- (72) Goddard, S. J.; Levitt, G. Substituted Isoindoles. *US Patent* **1978**, 4, 120, 693. CA: 90: 38788.

JM990345W